

SANDPILES AND DOMINOS

LAURA FLORESCU, DANIELA MORAR, DAVID PERKINSON, NICK SALTER,
AND TIANYUAN XU

ABSTRACT. We consider the subgroup of the abelian sandpile group of the grid graph consisting of configurations of sand that are symmetric with respect to central vertical and horizontal axes. We show that the size of this group is (i) the number of domino tilings of a corresponding weighted rectangular checkerboard; (ii) a product of special values of Chebyshev polynomials; and (iii) a double-product whose factors are sums of squares of values of trigonometric functions. We provide a new derivation of the formula due to Kasteleyn and to Temperley and Fisher for counting the number of domino tilings of a $2m \times 2n$ rectangular checkerboard and a new way of counting the number of domino tilings of a $2m \times 2n$ checkerboard on a Möbius strip.

1. INTRODUCTION

This paper relates the Abelian Sandpile Model (ASM) on a grid graph to domino tilings of checkerboards. The ASM is, roughly, a game in which one places grains of sand on the vertices of a graph, Γ , whose vertices and edges we assume to be finite in number. If the amount of sand on a vertex reaches a certain threshold, the vertex becomes unstable and fires, sending a grain of sand to each of its neighbors. Some of these neighbors, in turn, may now be unstable. Thus, adding a grain of sand to the system may set off a cascade of vertex firings. The resulting “avalanche” eventually subsides, even though our graph is finite, since the system is not conservative: there is a special vertex that serves as a sink, absorbing any sand that reaches it. It is assumed that every vertex is connected to the sink by a path of edges, so as a consequence, every pile of sand placed on the graph stabilizes after a finite number of vertex firings. It turns out that this stable state only depends on the initial configuration of sand, not on the order of the firings of unstable vertices, which accounts for the use of the word “abelian.”

Now imagine starting with no sand on Γ then repeatedly choosing a vertex at random, adding a grain of sand, and allowing the pile of sand to stabilize. In the resulting sequence of configurations of sand, certain configurations will appear infinitely often. These are the so-called “recurrent” configurations. A basic theorem in the theory of sandpiles is that the collection of recurrent configurations forms an additive group, where addition is defined as vertex-wise addition of grains of sand, followed by stabilization. This group is called the *sandpile group* or *critical group* of Γ . Equivalent versions of the sandpile group have arisen independently. For a history and as a general reference, see [14].

In their seminal 1987 paper, Bak, Tang, and Wiesenfeld (BTW), [1], studied sandpile dynamics in the case of what we call the *sandpile grid graph*. To construct the $m \times n$ sandpile grid graph, start with the ordinary grid graph with vertices

$[m] \times [n]$ and edges $\{(i, j), (i', j')\}$ such that $|i - i'| + |j - j'| = 1$. Then add a new vertex to serve as a sink, and add edges from the boundary vertices to the sink so that each vertex on the grid has degree 4. Thus, corner vertices have two edges to the sink (assuming m and n are greater than 1), as on the left in Figure 6. Dropping one grain of sand at a time onto a sandpile grid graph and letting the system stabilize, BTW experimentally finds that eventually the system evolves into a barely stable “self-organized critical” state. This critical state is characterized by the property that the sizes of avalanches caused by dropping a single grain—measured either temporally (by the number of ensuing vertex firings) or spatially (by the number of different vertices that fire)—obey a power law. The power-laws observed by BTW in the case of some sandpile grid graphs have not yet been proven.

The ASM, due to Dhar [8], is a generalization of the BTW model to a wider class of graphs. It was Dhar who made the key observation of its abelian property and who coined the term “sandpile group” for the collection of recurrent configurations of sand. In terms of the ASM, the evolution to a critical state observed by BTW comes from the fact that by repeatedly adding a grain of sand to a graph and stabilizing, one eventually reaches a configuration that is recurrent. Past this point, each configuration reached by adding sand and stabilizing is again recurrent.

Other work on ASM and statistical physics includes [12]. In addition, the ASM has been shown to have connections with a wide range of mathematics, including algebraic geometry and commutative algebra ([2], [10], [7], [23], [22], [34]), pattern formation ([30],[31],[33], [32],[36]), potential theory ([3],[4],[20]), combinatorics ([15], [16],[26], [35]), and number theory ([28]). The citations here are by no means exhaustive. One might argue that the underlying reason for these connections is that the firing rules for the ASM encode the discrete Laplacian matrix of the graph (as explained in Section 2). Thus, the ASM is a means of realizing the dynamics implicit in the discrete Laplacian.

The initial motivation for our work was a question posed to the second and third authors by Irena Swanson. She was looking at an online computer program [24] for visualizing the ASM on a sandpile grid graph. By pushing a button, the program adds one grain of sand to each of the nonsink vertices then stabilizes the resulting configuration. Swanson asked, “Starting with no sand, how many times would I need to push this button to get the identity of the sandpile group?” A technicality arises here: the configuration consisting of one grain of sand on each vertex is not recurrent, hence, not in the group. However, the all-2s configuration, having two grains at each vertex, is recurrent. So for the sake of this introduction, we reword the question as: “What is the order of the all-2s configuration?”

Looking at data (cf. Section 5, Table 1), one is naturally led to the special case of the all-2s configuration on the $2n \times 2n$ sandpile grid graph, which we denote by $\vec{2}_{2n \times 2n}$. The orders for $\vec{2}_{2n \times 2n}$ for $n = 1, \dots, 5$ are

$$1, 3, 29, 901, 89893.$$

Plugging these numbers into the Online Encyclopedia of Integer Sequences yields a single match, sequence A065072 ([29]): the sequence of odd integers $(a_n)_{n \geq 1}$ such that $2^n a_n^2$ is the number of domino tilings of the $2n \times 2n$ checkerboard.¹ (Some

¹By a *checkerboard* we mean a rectangular array of squares. A *domino* is a 1×2 or 2×1 array of squares. A *domino tiling* of a checkerboard consists of covering all of the squares of the checkerboard—each domino covers two—with dominos.

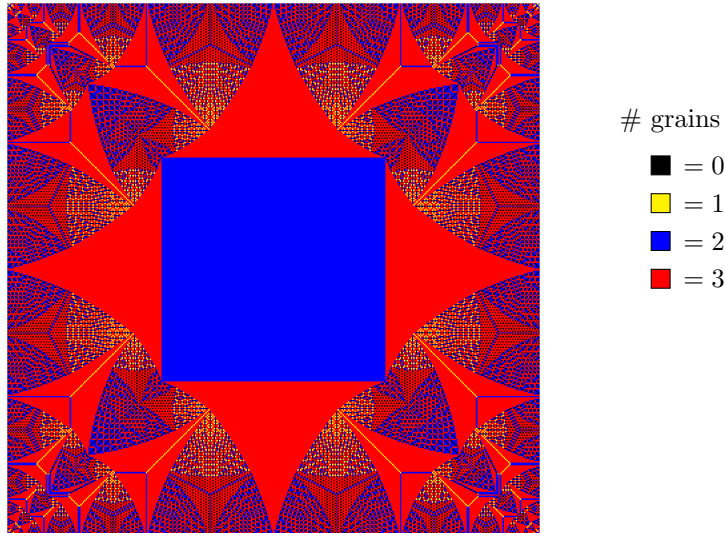


FIGURE 1. Identity element for the sandpile group of the 400×400 sandpile grid graph.

background on this sequence is included in Section 5.) So we conjectured that the order of $\vec{2}_{2n \times 2n}$ is equal to a_n , and trying to prove this is what first led to the ideas presented here. Difficulty in finishing our proof of the conjecture led to further computation, at which time we (embarrassingly) found that the order of $\vec{2}_{2n \times 2n}$ for $n = 6$ is, actually, $5758715 = a_6/5$. Thus, the conjecture is false, and there are apparently at least two natural sequences that start $1, 3, 29, 901, 89893!$ Theorem 5.5 shows that the cyclic group generated by $\vec{2}_{2n \times 2n}$ is isomorphic to a subgroup of a sandpile group whose order is a_n , and therefore the order of $\vec{2}_{2n \times 2n}$ divides a_n . We do not know when equality holds, and we have not yet answered Irena Swanson's question.

On the other hand, further experimentation using the mathematical software Sage led us to a more fundamental connection between the sandpile group and domino tilings of the grid graph. The connection is due to a property that is a notable feature of the elements of the subgroup generated by the all-2s configuration—*symmetry* with respect to the central horizontal and vertical axes. The recurrent identity element for the sandpile grid graph, as exhibited in Figure 1, also has this symmetry.² If Γ is any graph equipped with an action of a finite group G , it is natural to consider the collection of G -invariant configurations. Proposition 2.6 establishes that the symmetric recurrent configurations form a subgroup of the sandpile group for Γ . The central purpose of this paper is to explain how symmetry links the sandpile group of the grid graph to domino tilings.

We now describe our main results. We study the recurrent configurations on the sandpile grid graph having $\mathbb{Z}/2 \times \mathbb{Z}/2$ symmetry with respect to the central

²For square grids, the identity is symmetric with respect to the dihedral group of order 8, but this phenomenon is of course not present in the rectangular grids that we also consider.

horizontal and vertical axes. The cases of even \times even-, even \times odd-, and odd \times odd-dimensional grids each have their own particularities, and so we divide their analysis into separate cases, resulting in Theorems 4.2, 4.5, and 4.10, respectively. In each case, we compute the number of symmetric recurrents as (i) the number of domino tilings of corresponding (weighted) rectangular checkerboards; (ii) a product of special values of Chebyshev polynomials; and (iii) a double-product whose factors are sums of squares of values of trigonometric functions.

For instance, of the 557,568,000 elements of the sandpile group of the 4×4 grid graph, only the 36 configurations displayed in Figure 8 are up-down and left-right symmetric. In accordance with Theorem 4.2,

$$\begin{aligned} 36 &= U_4(i \cos(\pi/5)) U_4(i \cos(2\pi/5)) \\ (1.1) \quad &= \prod_{h=1}^2 \prod_{k=1}^2 (4 \cos^2(h\pi/5) + 4 \cos^2(k\pi/5)), \end{aligned}$$

where $U_4(x) = 16x^4 - 12x^2 + 1$ is the fourth Chebyshev polynomial of the second kind.

The double-product in equation (1.1) is an instance of the famous formula due to Kasteleyn [18] and to Temperley and Fisher [39] for the number of domino tilings of a $2m \times 2n$ checkerboard:

$$\prod_{h=1}^m \prod_{k=1}^n \left(4 \cos^2 \frac{h\pi}{2m+1} + 4 \cos^2 \frac{k\pi}{2n+1} \right),$$

for which Theorem 4.2 provides a new proof.

In the case of the even \times odd grid, there is an extra “twist”: the double-product in Theorem 4.5 for the even \times odd grid is (a slight re-writing of) the formula of Lu and Wu [21] for the number of domino tilings of a checkerboard on a Möbius strip.

To sketch the main idea behind the proofs of these theorems, suppose a group G acts on a graph Γ with fixed sink vertex (cf. Section 2.2). To study symmetric configurations with respect to the action of G , one considers a new firing rule in which a vertex only fires simultaneously with all other vertices in its orbit under G . This new firing rule can be encoded in an $m \times m$ matrix D where m is the number of orbits of nonsink vertices of G . We show in Corollary 2.11 that $\det(D)$ is the number of symmetric recurrents on G . Suppose, as is the case for sandpile grid graphs, that either D or its transpose happens to be the (reduced) Laplacian of an associated graph Γ' . The nonsink vertices correspond to the orbits of vertices of the original graph. The well-known matrix-tree theorem says that the determinant of D is the number of spanning trees of Γ' . Then the generalized Temperley bijection [19] says these spanning trees correspond with perfect matchings of a third graph Γ'' . In this way, the symmetric recurrents on Γ can be put into correspondence with the perfect matchings of Γ'' . In the case where Γ is a sandpile grid graph, Γ'' is a weighted grid graph, and perfect matchings of it correspond to weighted tilings of a checkerboard. Also, in this case, the matrix D has a nice block triangular form (cf. Lemma 4.1), which leads to a recursive formula for its determinant and a connection with Chebyshev polynomials.

OUTLINE

1 Introduction.**2 Sandpiles.**

2.1 Basics. A summary of the basic theory of sandpiles needed for this paper.

2.2 Symmetric configurations. Group actions on sandpile graphs. Proposition 2.6 shows that the collection of symmetric recurrents forms a subgroup of the sandpile group. We introduce the *symmetrized reduced Laplacian* operator, $\tilde{\Delta}^G$, and use it to determine the structure of this subgroup in Proposition 2.10. An important consequence is Corollary 2.11, which shows that the number of symmetric recurrents equals $\det \tilde{\Delta}^G$.

3 Matchings and trees. A description of the generalized Temperley bijection [19] between weighted spanning trees of a planar graph and weighted perfect matchings of a related graph.

4 Symmetric recurrents on the sandpile grid graph. We count symmetric recurrents on sandpile grid graphs using weighted tilings of checkerboards, Chebyshev polynomials, and Kasteleyn-type formulae. The problem is split into three cases.

4.1 Some tridiagonal matrices. A summary of some properties of Chebyshev polynomials and a proof Lemma 4.1, which calculates the determinant of a certain form of tridiagonal block matrix. The symmetrized reduced Laplacian matrices for the three classes of sandpile grid graphs, below, have this form. Their determinants count symmetric recurrents.

4.2 Symmetric recurrents on a $2m \times 2n$ sandpile grid graph. See Theorem 4.2.

4.3 Symmetric recurrents on a $2m \times (2n - 1)$ sandpile grid graph. See Theorem 4.5.

4.4 Symmetric recurrents on a $(2m - 1) \times (2n - 1)$ sandpile grid graph. See Theorem 4.10.

5 The order of the all-twos configuration. Corollary 5.6: the order of the all-2s configuration on the $2n \times 2n$ sandpile grid divides the odd number a_n such that $2^n a_n^2$ is the number of domino tilings of the $2n \times 2n$ checkerboard.

6 Conclusion. A list of open problems.

Acknowledgments. We thank Irena Swanson for providing initial motivation. We thank the organizers of the Special Session on Laplacian Growth at the Joint Mathematics Meeting, New Orleans, LA, 2011 at which some of this work was presented, and we thank Lionel Levine, in particular, for encouragement and helpful remarks. Finally, we would like to acknowledge the mathematical software Sage [38] and the Online Encyclopedia of Integer Sequences [29] which were both essential for our investigations.

2. SANDPILES

2.1. Basics. In this section, we recall the basic theory of sandpile groups. The reader is referred to [14] for details. Let $\Gamma = (V, E, \text{wt}, s)$ be a directed graph with vertices V , edges E , edge-weight function $\text{wt}: V \times V \rightarrow \mathbb{N} := \{0, 1, 2, \dots\}$, and special vertex $s \in V$. For each pair $v, w \in V$, we think of $\text{wt}(v, w)$ as the number

of edges running from v to w . In particular, $\text{wt}(v, w) > 0$ if and only if $(v, w) \in E$. The vertex s is called the *sink* of Γ , and it is assumed that each vertex of Γ has a directed path to s . Let $\tilde{V} := V \setminus \{s\}$ be the set of non-sink vertices. A (*sandpile*) *configuration* on Γ is an element of $\mathbb{N}\tilde{V}$, the free monoid on \tilde{V} . If $c = \sum_{v \in \tilde{V}} c_v v$ is a configuration, we think of each component, c_v , as a number of grains of sand stacked on vertex v . The vertex $v \in \tilde{V}$ is *unstable* in c if $c_v \geq \text{outdeg}(v)$ where $\text{outdeg}(v) := \sum_{w \in \tilde{V}} \text{wt}(v, w)$, is the *out-degree* of v , i.e., the number of directed edges emanating from v . If v is unstable in c , we may *fire (topple)* c at v to get a new configuration c' defined for each $w \in \tilde{V}$ by

$$c'_w = \begin{cases} c_v - \text{outdeg}(v) + \text{wt}(v, v) & \text{if } w = v, \\ c_w + \text{wt}(v, w) & \text{if } w \neq v. \end{cases}$$

In other words,

$$c' = c - \text{outdeg}(v)v + \sum_{w \in \tilde{V}} \text{wt}(v, w) w.$$

If the configuration \tilde{c} is obtained from c by a sequence of firings of unstable vertices, we write

$$c \rightarrow \tilde{c}.$$

Since each vertex has a path to the sink, s , it turns out that by repeatedly firing unstable vertices each configuration relaxes to a stable configuration. Moreover, this stable configuration is independent of the ordering of firing of unstable vertices. Thus, we may talk about *the* stabilization of a configuration c , which we denote by c° . Define the binary operation of *stable addition* on the set of all configurations as component-wise addition followed by stabilization. In other words, the stable addition of configurations a and b is given by

$$(a + b)^\circ.$$

Let \mathcal{M} denote the collection of stable configurations on Γ . Then stable addition restricted to \mathcal{M} makes \mathcal{M} into a commutative monoid.

A configuration c on Γ is *recurrent* if: (1) it is stable, and (2) given any configuration a , there is a configuration b such that $(a + b)^\circ = c$. The *maximal stable configuration*, c_{\max} , is defined by

$$c_{\max} := \sum_{v \in \tilde{V}} (\text{outdeg}(v) - 1) v.$$

It turns out that the collection of recurrent configurations forms a principal semi-ideal of \mathcal{M} generated by c_{\max} . This means that the recurrent configurations are exactly those obtained by adding sand to the maximal stable configuration and stabilizing. Further, the collection of recurrent configurations forms a group, $\mathcal{S}(\Gamma)$, called the *sandpile group* for Γ . Note that the identity for $\mathcal{S}(\Gamma)$ is not usually the zero-configuration, $\vec{0} \in \mathbb{N}\tilde{V}$.

For an undirected graph, i.e., a graph for which $\text{wt}(u, v) = \text{wt}(v, u)$ for each pair of vertices u and v , one may use the *burning algorithm*, due to Dhar [9], to determine whether a configuration is recurrent (for a generalization to directed graphs, see [37]):

Theorem 2.1 ([9],[14, Lemma 4.1]). *Let c be a stable configuration on an undirected graph Γ . Define the burning configuration on Γ to be the configuration obtained by*

firing the sink vertex:

$$b := \sum_{v \in \tilde{V}} \text{wt}(s, v) v.$$

Then in the stabilization of $b + c$, each vertex fires at most once, and the following are equivalent:

- (1) c is recurrent;
- (2) $(b + c)^\circ = c$;
- (3) in the stabilization of $b + c$, each non-sink vertex fires.

Define the *proper Laplacian*, $L: \mathbb{Z}^V \rightarrow \mathbb{Z}^V$, of Γ by

$$L(f)(v) := \sum_{w \in V} \text{wt}(v, w)(f(v) - f(w))$$

for each function $f \in \mathbb{Z}^V$. Taking the \mathbb{Z} -dual (applying the functor $\text{Hom}(\cdot, \mathbb{Z})$) gives the mapping of free abelian groups

$$\Delta: \mathbb{Z}V \rightarrow \mathbb{Z}V$$

defined on vertices $v \in V$ by

$$\Delta(v) = \text{outdeg}(v) v - \sum_{w \in V} \text{wt}(v, w) w.$$

We call Δ the *Laplacian* of Γ . Restricting Δ to $\mathbb{Z}\tilde{V}$ and setting the component of s equal to 0 gives the *reduced Laplacian*, $\tilde{\Delta}: \mathbb{Z}\tilde{V} \rightarrow \mathbb{Z}\tilde{V}$. If v is an unstable vertex in a configuration c , firing v gives the new configuration

$$c - \tilde{\Delta}v.$$

There is a well-known isomorphism

$$(2.1) \quad \begin{aligned} \mathcal{S}(\Gamma) &\rightarrow \mathbb{Z}\tilde{V}/\text{image}(\tilde{\Delta}) \\ c &\mapsto c. \end{aligned}$$

While there may be many stable configurations in each equivalence class of $\mathbb{Z}\tilde{V}$ modulo $\text{image}(\tilde{\Delta})$, there is only one that is recurrent. For instance, the recurrent element in the equivalence class of $\tilde{0}$ is the identity of $\mathcal{S}(\Gamma)$.

A *spanning tree of Γ rooted at s* is a directed subgraph containing all the vertices, having no directed cycles, and for which s has no out-going edges while every other vertex has exactly one out-going edge. The weights of the edges of a spanning tree are the same as they are for Γ , and the *weight* of a spanning tree is the product of the weights of its edges. The matrix-tree theorem says the sum of the weights of the set of all spanning trees of Γ rooted at s is equal to $\det \tilde{\Delta}$, the determinant of the reduced Laplacian. It then follows from (2.1) that the number of elements of the sandpile group is also the sum of the weights of the spanning trees rooted at s .

2.2. Symmetric configurations. Preliminary versions of the results in this section appear in [11]. Let G be a finite group. An *action* of G on Γ is an action of G on V fixing s , sending edges to edges, and preserving edge-weights. In detail, it is a mapping

$$\begin{aligned} G \times V &\rightarrow V \\ (g, v) &\mapsto gv \end{aligned}$$

satisfying

- (1) if e is the identity of G , then $ev = v$ for all $v \in V$;
- (2) $g(hv) = (gh)v$ for all $g, h \in G$ and $v \in V$;
- (3) $gs = s$ for all $g \in G$;
- (4) if $(v, w) \in E$, then $(gv, gw) \in E$ and both edges have the same weight.

Note that these conditions imply that $\text{outdeg}(v) = \text{outdeg}(gv)$ for all $v \in V$ and $g \in G$. For the rest of this section, let G be a group acting on Γ .

By linearity, the action of G extends to an action on $\mathbb{N}V$ and $\mathbb{Z}V$. Since G fixes the sink, G acts on configurations and each element of G induces an automorphism of $\mathcal{S}(\Gamma)$ (cf. 2.3). We say a configuration c is *symmetric* (with respect to the action by G) if $gc = c$ for all $g \in G$.

Proposition 2.2. *The action of G commutes with stabilization. That is, if c is any configuration on Γ and $g \in G$, then $g(c^\circ) = (gc)^\circ$.*

Proof. Suppose that c is stabilized by firing the sequence of vertices v_1, \dots, v_t . Then

$$c^\circ = c - \sum_{i=1}^t \tilde{\Delta}v_i.$$

At the k -th step in the stabilization process, c has relaxed to the configuration $c' := c - \sum_{i=1}^k \tilde{\Delta}v_i$. A vertex v is unstable in c' if and only if gv is unstable in $gc' = gc - \sum_{i=1}^k \tilde{\Delta}(gv_i)$. Thus, we can fire the sequence of vertices gv_1, \dots, gv_t in gc , resulting in the stable configuration

$$(gc)^\circ = gc - \sum_{i=1}^t \tilde{\Delta}(gv_i).$$

□

Corollary 2.3. *The action of G preserves recurrent configurations, i.e., if c is a recurrent configuration and $g \in G$, then gc is recurrent.*

Proof. If c is recurrent, we can find a configuration b such that $c = (b + c_{\max})^\circ$. Then,

$$gc = g(b + c_{\max})^\circ = (gb + gc_{\max})^\circ = (gb + c_{\max})^\circ.$$

Hence, gc is recurrent. □

Corollary 2.4. *If c is a symmetric configuration, then so is its stabilization.*

Proof. For all $g \in G$, if $gc = c$, then $g(c^\circ) = (gc)^\circ = c^\circ$. □

Remark 2.5. In fact, if c is a symmetric configuration, one may find a sequence of symmetric configurations, c_1, \dots, c_t with $c_t = c^\circ$ such that $c \rightarrow c_1 \rightarrow \dots \rightarrow c_t$. This follows since in a symmetric configuration a vertex v is unstable if and only if gv is unstable for all $g \in G$. To construct c_{i+1} from c_i , simultaneously fire all unstable vertices of c_i (an alternative is to pick any vertex v , unstable in c_i , and simultaneously fire the vertices in $\{gv : g \in G\}$).

Proposition 2.6. *The collection of symmetric recurrent configurations forms a subgroup of the sandpile group $\mathcal{S}(\Gamma)$.*

Proof. Since the group action respects addition in $\mathbb{N}\tilde{V}$ and stabilization, the sum of two symmetric recurrent configurations is again symmetric and recurrent. There is at least one symmetric recurrent configuration, namely, c_{\max} . Since the sandpile group is finite, it follows that these configurations form a subgroup. □

Notation 2.7. The subgroup of symmetric recurrent configurations on Γ with respect to the action of the group G is denoted $\mathcal{S}(\Gamma)^G$.

Proposition 2.8. *If c is symmetric and recurrent then $c = (a + c_{\max})^\circ$ for some symmetric configuration a .*

Proof. By [37] there exists an element b in the image of $\tilde{\Delta}$ such that: (1) $b_v \geq 0$ for all $v \in \tilde{V}$, and (2) for each vertex $w \in \tilde{V}$, there is a directed path to w from some $v \in \tilde{V}$ such that $b_v > 0$, i.e., from some v in the *support* of b . (If Γ is undirected, one may find such a b by applying $\tilde{\Delta}$ to the vector whose components are all 1s). Define

$$b^G = \sum_{g \in G} gb.$$

Then b^G is symmetric and equal to zero modulo the image of $\tilde{\Delta}$. Take a large positive integer N and consider Nb^G , the vertex-wise addition of b^G with itself N times without stabilizing. Every vertex of Γ is connected by a path from a vertex in the support of b , and hence, the same is true of Nb^G . Thus, by choosing N large enough and by firing symmetric vertices of Nb^G , we obtain a symmetric configuration b' such that $b'_v \geq c_{\max, v}$ for all v and such that b' is zero modulo the image of $\tilde{\Delta}$. Define $a = b' - c_{\max} + c$, by construction a symmetric configuration. The unique recurrent element in the equivalence class of $b' + c$ modulo the image of $\tilde{\Delta}$ is c . Therefore,

$$(a + c_{\max})^\circ = (b' + c)^\circ = c.$$

□

The *orbit* of $v \in V$ under G is the set

$$Gv = \{gv : g \in G\}.$$

Let $\mathcal{O} = \mathcal{O}(\Gamma, G) = \{Gv : v \in \tilde{V}\}$ denote the set of orbits of the non-sink vertices. The *symmetrized reduced Laplacian* is the \mathbb{Z} -linear mapping

$$(2.2) \quad \tilde{\Delta}^G: \mathbb{Z}\mathcal{O} \rightarrow \mathbb{Z}\mathcal{O}$$

such that for all $v, w \in \tilde{V}$, the Gw -th component of $\tilde{\Delta}^G(Gv)$ is

$$\left(\sum_{u \in Gv} \tilde{\Delta}(u) \right)_w.$$

Remark 2.9. If $c \in \mathbb{Z}\tilde{V}$ is symmetric, then define $[c] \in \mathbb{Z}\mathcal{O}$ by $[c]_{Gv} := c_v$ for all $v \in \tilde{V}$, thus obtaining a bijection between symmetric elements of $\mathbb{Z}\tilde{V}$ and $\mathbb{Z}\mathcal{O}$. The mapping $\tilde{\Delta}^G$ is defined so that if c is a symmetric configuration and $v \in \tilde{V}$, then $[c] - \tilde{\Delta}^G(Gv)$ is the element of $\mathbb{Z}\mathcal{O}$ corresponding to

$$c - \tilde{\Delta}(\sum_{w \in Gv} w),$$

the symmetric configuration obtained from c by firing all vertices in the orbit of v .

For the following let $r: \mathbb{Z}\tilde{V}/\text{image}(\tilde{\Delta}) \rightarrow \mathcal{S}(\Gamma)$ denote the inverse of the isomorphism in (2.1).

Proposition 2.10. *There is an isomorphism of groups,*

$$\phi: \mathbb{Z}\mathcal{O}/\text{image}(\tilde{\Delta}^G) \rightarrow \mathcal{S}(\Gamma)^G,$$

determined by $Gv \mapsto r(\sum_{w \in Gv} w)$ for $v \in \tilde{V}$.

Proof. The homomorphism $\lambda: \mathbb{Z}\mathcal{O} \rightarrow \mathbb{Z}\tilde{V}$ determined by

$$\lambda(Gv) := \sum_{w \in Gv} w$$

for $v \in \tilde{V}$ induces the (well-defined) mapping

$$\Lambda: \mathbb{Z}\mathcal{O}/\text{image}(\tilde{\Delta}^G) \rightarrow \mathbb{Z}\tilde{V}/\text{image}(\tilde{\Delta}).$$

To see that the image of $r \circ \Lambda$ is symmetric, consider the symmetric configuration $|\mathcal{S}(\Gamma)| \cdot c_{\max} \in \mathbb{Z}\tilde{V}$, a configuration in the image of $\tilde{\Delta}$. For each $v \in \tilde{V}$,

$$\phi(Gv) = r(\Lambda(Gv)) = (|\mathcal{S}(\Gamma)| \cdot c_{\max} + \lambda(Gv))^\circ,$$

which is symmetric by Corollary 2.4.

The mapping $c \mapsto [c]$, introduced in Remark 2.9, is a left inverse to λ . Thus, if $c \in \mathcal{S}(\Gamma)^G$, then $\phi([c]) = c$, and hence ϕ is surjective. To show that ϕ is injective, it suffices to show that Λ is injective. So suppose that $a = \lambda(o)$ for some $o \in \mathbb{Z}\mathcal{O}$ and that $a = \tilde{\Delta}(b)$ for some $b \in \mathbb{Z}\tilde{V}$. Fix $g \in G$, and consider the isomorphism $g: \mathbb{Z}\tilde{V} \rightarrow \mathbb{Z}\tilde{V}$ determined by the action of g on vertices. A straightforward calculation shows that $\tilde{\Delta} = g\tilde{\Delta}g^{-1}$. It follows that

$$\tilde{\Delta}(b) = a = ga = g\tilde{\Delta}b = (g\tilde{\Delta}g^{-1})(gb) = \tilde{\Delta}(gb).$$

Since $\tilde{\Delta}$ is invertible, it follows that $b = gb$ for all $g \in G$, i.e., b is symmetric. Hence, $o = [a] = \tilde{\Delta}^G([b])$, as required. \square

Corollary 2.11. *The number of symmetric recurrent configurations is*

$$|\mathcal{S}(\Gamma)^G| = \det \tilde{\Delta}^G.$$

Remark 2.12. We have not assumed that the action of G on Γ is faithful. If K is the kernel of the action of G , then $\mathcal{O}(\Gamma, G) = \mathcal{O}(\Gamma, G/K)$ and $\mathcal{S}^G = \mathcal{S}^{G/K}$. We also have $\tilde{\Delta}^G = \tilde{\Delta}^{G/K}$.

Example 2.13. Consider the graph Γ of Figure 2 with sink s and with each edge having weight 1.

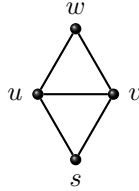


FIGURE 2. The graph Γ for Example 2.13.

Let $G = \{e, g\}$ be the group of order 2 with identity e . Consider the action of G on Γ for which g swaps vertices u and v and fixes vertices w and s . Ordering the vertices of Γ as u, v, w and ordering the orbits, \mathcal{O} , as Gu, Gv , the reduced Laplacian and the symmetrized reduced Laplacian for Γ become

$$\tilde{\Delta} = \begin{bmatrix} 3 & -1 & -1 \\ -1 & 3 & -1 \\ -1 & -1 & 2 \end{bmatrix}, \quad \tilde{\Delta}^G = \begin{bmatrix} 2 & -1 \\ -2 & 2 \end{bmatrix},$$

$u \quad v \quad w$ $Gu \quad Gw$

where we have labeled the columns by their corresponding vertices or orbits for convenience. To illustrate how one would compute the columns of the symmetrized reduced Laplacian in general, consider the column of $\tilde{\Delta}^G$ corresponding to $Gu = \{u, v\}$. It was computed by first adding the u - and v -columns of $\tilde{\Delta}$ to get the 3-vector $\ell = (2, 2, -2)$, then taking the u and w components of ℓ since u and w were chosen as orbit representatives.

There are $8 = \det \tilde{\Delta}$ recurrent elements (c_u, c_v, c_w) of Γ :

$$(0, 2, 1), (1, 2, 0), (1, 2, 1), (2, 0, 1), (2, 1, 0), (2, 1, 1), (2, 2, 0), (2, 2, 1),$$

and $(2, 2, 0)$ is the identity of $\mathcal{S}(\Gamma)$. In accordance with Corollary 2.11, there are $2 = \det \tilde{\Delta}^G$ symmetric recurrent elements: $(2, 2, 0)$ and $(2, 2, 1)$. \square

3. MATCHINGS AND TREES

In this section, assume that $\Gamma = (V, E, \text{wt}, s)$ is embedded in the plane, and fix a face f_s containing the sink vertex, s . In §4 and §5, we always take f_s to be the unbounded face. We recall the generalized Temperley bijection, due to [19], between directed spanning trees of Γ rooted at s and perfect matchings of a related weighted undirected graph, $\mathcal{H}(\Gamma)$. (The graph $\mathcal{H}(\Gamma)$ would be denoted $\mathcal{H}(s, f_s)$ in [19].)

It is sometimes convenient to allow an edge $e = (u, v)$ to be represented in the embedding by distinct weighted edges e_1, \dots, e_k , each with tail u and head v , such that $\sum_{i=1}^k \text{wt}(e_i) = \text{wt}(e)$. Also, we would like to be able to embed a pair of oppositely oriented edges between the same vertices so that they coincide in the plane. For these purposes then, we work in the more general category of weighted directed *multi*-graphs by allowing E to be a *multiset* of edges in which an edge e with endpoints u and v is represented as the set $e = \{u, v\}$ with a pair of weights $\text{wt}(e, (u, v))$ and $\text{wt}(e, (v, u))$, at least one of which is nonzero. Each edge in the embedding is then represented by a double-headed arrow with two weight labels (the label $\text{wt}(e, (u, v))$ being placed next to the head vertex, v). Figure 3 shows a pair of edges $e = \{u, v\}$ and $e' = \{u, v\}$ where $\text{wt}(e, (u, v)) = 2$, $\text{wt}(e, (v, u)) = 0$, $\text{wt}(e', (u, v)) = 3$, and $\text{wt}(e', (v, u)) = 1$. The top edge, e , represents a single directed edge (u, v) of weight 2, and the bottom edge represents a pair of directed edges of weights 3 and 1. The two edges combine to represent a pair of directed edges, (u, v) of weight 5 and (v, u) of weight 1.

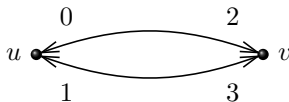


FIGURE 3. Edges for a planar embedding of a weighted directed graph.

The rough idea of the construction of the weighted undirected graph $\mathcal{H}(\Gamma)$ is to overlay the embedded graph Γ with its dual, forgetting the orientation of the

edges and introducing new vertices where their edges cross. Then remove s and the vertex corresponding to the chosen face f_s , and remove their incident edges. In detail, the vertices of $\mathcal{H}(\Gamma)$ are

$$V_{\mathcal{H}(\Gamma)} := \{t_v : v \in V \setminus \{s\}\} \cup \{t_e : e \in E\} \cup \{t_f : f \in F \setminus \{f_s\}\},$$

where F is the set of faces of Γ , including the unbounded face, and the edges of $\mathcal{H}(\Gamma)$ are

$$E_{\mathcal{H}(\Gamma)} := \{\{t_u, t_e\} : u \in V \setminus \{s\}, u \in e \in E\} \cup \{\{t_e, t_f\} : e \in E, e \in f \in F \setminus \{f_s\}\}.$$

The weight of each edge of the form $\{t_u, t_e\}$ with $e = \{u, v\} \in E$ is defined to be $\text{wt}(e, (u, v))$, and the weight of each edge of the form $\{t_e, t_f\}$ with $f \in F$ is defined to be 1.

Figure 4 depicts a graph Γ embedded in the plane (for which the multiset E is actually just a set). The graph displayed in the middle is the superposition of Γ with its dual, Γ^\perp . The unbounded face is chosen as f_s . For convenience, its corresponding vertex is omitted from the middle graph, and its incident edges are only partially drawn.

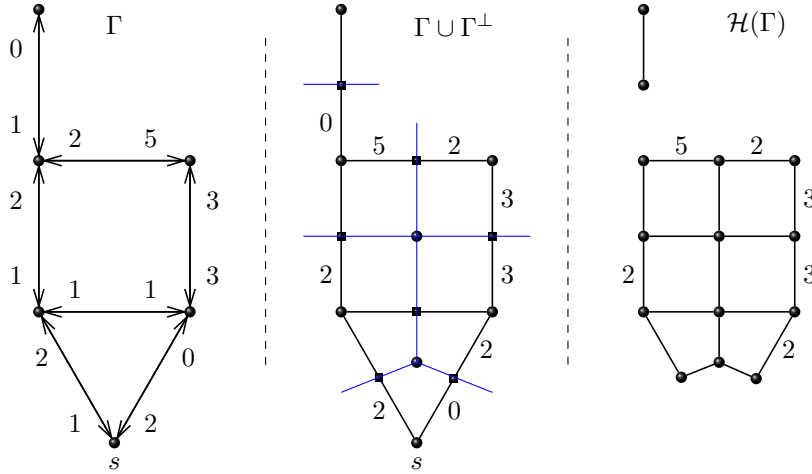


FIGURE 4. Construction of $\mathcal{H}(\Gamma)$. (Unlabeled edges have weight 1.)

A *perfect matching* of a weighted undirected graph is a subset of its edges such that each vertex of the graph is incident with exactly one edge in the subset. The *weight* of a perfect matching is the product of the weights of its edges.

We now describe the weight-preserving bijection between perfect matchings of $\mathcal{H}(\Gamma)$ and directed spanning trees of Γ rooted at s due to [19]. Let T be a directed spanning tree of Γ rooted at s , and let \tilde{T} be the corresponding directed spanning tree of Γ^\perp , the dual of Γ , rooted at f_s . (The tree \tilde{T} is obtained by properly orienting the edges of Γ^\perp that do not cross edges of T in $\Gamma \cup \Gamma^\perp$.) The perfect matching of $\mathcal{H}(\Gamma)$ corresponding to T consists of the following:

- (1) an edge $\{t_u, t_e\}$ of weight $\text{wt}(e)$ for each $e = (u, v) \in T$;
- (2) an edge $\{t_f, t_e\}$ of weight 1 for each $\tilde{e} = (f, f') \in \tilde{T}$, where e is the edge in Γ that crossed by \tilde{e} .

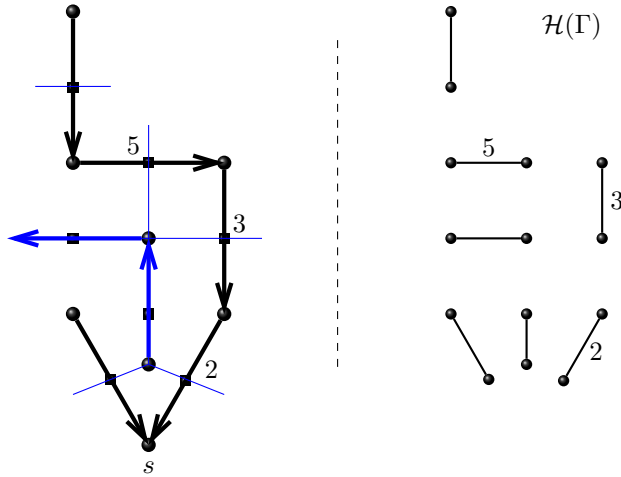


FIGURE 5. A spanning tree of Γ determines a dual spanning tree for Γ^\perp and a perfect matching for $\mathcal{H}(\Gamma)$. (See Figure 4. Unlabeled edges have weight 1.)

See Figure 5 for an example continuing the example from Figure 4.

As discussed in [19], although $\mathcal{H}(\Gamma)$ depends on the embedding of Γ and on the choice of f_s , the number of spanning trees of Γ rooted at s (and hence, the number of perfect matchings of $\mathcal{H}(\Gamma)$), counted according to weight, does not change. In what follows, we will always choose f_s to be the unbounded face.

4. SYMMETRIC RECURRENTS ON THE SANDPILE GRID GRAPH

The *ordinary $m \times n$ grid graph* is the undirected graph $\Gamma_{m \times n}$ with vertices $[m] \times [n]$ and edges $\{(i, j), (i', j')\}$ such that $|i - i'| + |j - j'| = 1$. The *$m \times n$ sandpile grid graph*, $\text{SF}_{m \times n}$, is formed from $\Gamma_{m \times n}$ by adding a (disjoint) sink vertex, s , then edges incident to s so that every non-sink vertex of the resulting graph has degree 4. For instance, each of the four corners of the sandpile grid graph shares an edge of weight 2 with s in the case where $m \geq 2$ and $n \geq 2$, as on the left in Figure 6.

We embed $\Gamma_{m \times n}$ in the plane as the standard grid with vertices arranged as in a matrix, with $(1, 1)$ in the upper left and (m, n) in the lower right. We embed $\text{SF}_{m \times n}$ similarly, but usually identify the sink vertex, s , with the unbounded face of $\Gamma_{m \times n}$ for convenience in drawing, as on the left-hand side in Figure 6. The edges leading to the sink are sometimes entirely omitted from the drawing, as in Figure 10.

In this section, *symmetric recurrent* will always refer to a recurrent element on $\text{SF}_{m \times n}$ with horizontal and vertical symmetry, i.e., an element of $\mathcal{S}(\text{SF}_{m \times n})^G$ where G is the Klein 4-group,

$$G = \langle \sigma, \tau : \sigma^2 = \tau^2 = 1, \sigma\tau = \tau\sigma \rangle,$$

acting on $\text{SF}_{m \times n}$ by

$$\sigma(i, j) = (i, n - j + 1), \quad \tau(i, j) = (m - i + 1, j), \quad \text{and } \sigma(s) = \tau(s) = s.$$

Our main goal in this section is to study the symmetric recurrent configurations on the sandpile grid graph. After collecting some basic facts about certain tridiagonal matrices, we divide the study into three cases: even \times even-, even \times odd-, and

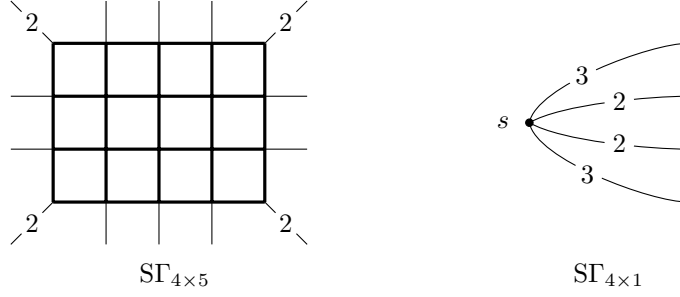


FIGURE 6. Two sandpile grid graphs. (The sink for $\text{SG}_{4 \times 5}$ is not drawn.)

odd \times odd-dimensional grids. In each case we provide a formula for the number of symmetric recurrences using Chebyshev polynomials and show how these configurations are related to domino tilings of various types of checkerboards.

4.1. Some tridiagonal matrices. Recall that *Chebyshev polynomials of the first kind* are defined by the recurrence

$$(4.1) \quad \begin{aligned} T_0(x) &= 1 \\ T_1(x) &= x \\ T_j(x) &= 2xT_{j-1}(x) - T_{j-2}(x) \quad \text{for } j \geq 2, \end{aligned}$$

and *Chebyshev polynomials of the second kind* are defined by

$$(4.2) \quad \begin{aligned} U_0(x) &= 1 \\ U_1(x) &= 2x \\ U_j(x) &= 2xU_{j-1}(x) - U_{j-2}(x) \quad \text{for } j \geq 2. \end{aligned}$$

Two references are [25] and [40].

It follows from the recurrences that these polynomials may be expressed as determinants of $j \times j$ tridiagonal matrices:

$$T_j(x) = \det \begin{bmatrix} x & 1 & & & \\ 1 & 2x & 1 & & \\ & 1 & 2x & 1 & \\ & & & \ddots & \\ & & & & 1 & 2x & 1 \\ & & & & & 1 & 2x \end{bmatrix}, \quad U_j(x) = \det \begin{bmatrix} 2x & 1 & & & \\ 1 & 2x & 1 & & \\ & 1 & 2x & 1 & \\ & & & \ddots & \\ & & & & 1 & 2x & 1 \\ & & & & & 1 & 2x \end{bmatrix},$$

and, hence, $T_j(-x) = (-1)^j T_j(x)$ and $U_j(-x) = (-1)^j U_j(x)$.

We have the well-known factorizations:

$$(4.3) \quad T_j(x) = 2^{j-1} \prod_{k=1}^j \left(x - \cos \left(\frac{(2k-1)\pi}{2j} \right) \right)$$

$$(4.4) \quad U_j(x) = 2^j \prod_{k=1}^j \left(x - \cos \left(\frac{k\pi}{j+1} \right) \right).$$

We will also use the following well-known identities:

$$(4.5) \quad T_{2j}(x) = T_j(2x^2 - 1) = (-1)^j T_j(1 - 2x^2)$$

$$(4.6) \quad 2T_j(x) = U_j(x) - U_{j-2}(x).$$

Corollary 2.11 will be used to count the symmetric recurrences on sandpile grid graphs. The form of the determinant that arises is treated by the following.

Lemma 4.1. *Let m and n be positive integers. Let A , B , and C be $n \times n$ matrices over the complex numbers, and let I_n be the $n \times n$ identity matrix. Define the $mn \times mn$ tridiagonal block matrix*

$$D(m) = \begin{bmatrix} A & -I_n & & & & \\ -I_n & A & -I_n & & & \\ & & \ddots & & & \\ & & & -I_n & A & -I_n \\ & & & & -C & B \end{bmatrix},$$

where the super- and sub-diagonal blocks are all $-I_n$ except for the one displayed block consisting of $-C$ and all omitted entries in the matrix are zero. Take $D(1) = B$. Then

$$\det D(m) = (-1)^n \det(T),$$

where

$$T = -B U_{m-1} \left(\frac{1}{2} A \right) + C U_{m-2} \left(\frac{1}{2} A \right),$$

letting $U_{-1}(x) := 0$.

Proof. The case $m = 1$ is immediate. For $m > 1$, Theorem 2 of [27] gives a formula for calculating the determinant of a general tridiagonal block matrix. In our case, it says

$$(4.7) \quad \det D(m) = (-1)^n \det E_{\mathbf{t}},$$

where $E_{\mathbf{t}}$ is the top-left block of size $n \times n$ of the matrix

$$E := \begin{bmatrix} -B & C \\ I_n & 0 \end{bmatrix} \begin{bmatrix} A & -I_n \\ I_n & 0 \end{bmatrix}^{m-2} \begin{bmatrix} A & I_n \\ I_n & 0 \end{bmatrix}.$$

Set $S_0 = I_n$, and for all positive integers j , define

$$S_j = \left(\begin{bmatrix} A & -I_n \\ I_n & 0 \end{bmatrix}^{j-1} \begin{bmatrix} A & I_n \\ I_n & 0 \end{bmatrix} \right)_{\mathbf{t}}$$

and

$$S'_j = \left(\begin{bmatrix} A & -I_n \\ I_n & 0 \end{bmatrix}^{j-1} \begin{bmatrix} A & I_n \\ I_n & 0 \end{bmatrix} \right)_{\mathbf{b}},$$

where the subscripts \mathbf{t} and \mathbf{b} denote taking the top-left and bottom-left blocks of size $n \times n$, respectively. It follows that

$$(4.8) \quad S_0 = I_n, \quad S_1 = A, \quad \text{and} \quad S_j = A S_{j-1} - S_{j-2} \text{ for } j \geq 2,$$

and

$$S'_j = S_{j-1} \text{ for all } j \geq 1.$$

By (4.2) and (4.8), $S_j = U_j(\frac{1}{2}A)$. Hence,

$$E_t = -B S_{m-1} + C S'_{m-1} = -B U_{m-1} \left(\frac{1}{2}A \right) + C U_{m-2} \left(\frac{1}{2}A \right),$$

as required. \square

4.2. Symmetric recurrences on a $2m \times 2n$ sandpile grid graph. A checkerboard is a rectangular array of squares. A domino is a 1×2 or 2×1 array of squares and, thus, covers exactly two adjacent squares of the checkerboard. A domino tiling of the checkerboard consists of placing non-overlapping dominos on the checkerboard, covering every square. As is usually done, and exhibited in Figure 7, we identify domino tilings of an $m \times n$ checkerboard with perfect matchings of $\Gamma_{m \times n}$. Figure 8 exhibits the 36 domino tilings of a 4×4 checkerboard.

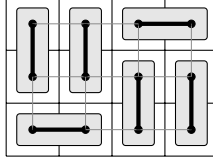


FIGURE 7. Correspondence between a perfect matching of $\Gamma_{3 \times 4}$ and a domino tiling of its corresponding checkerboard.

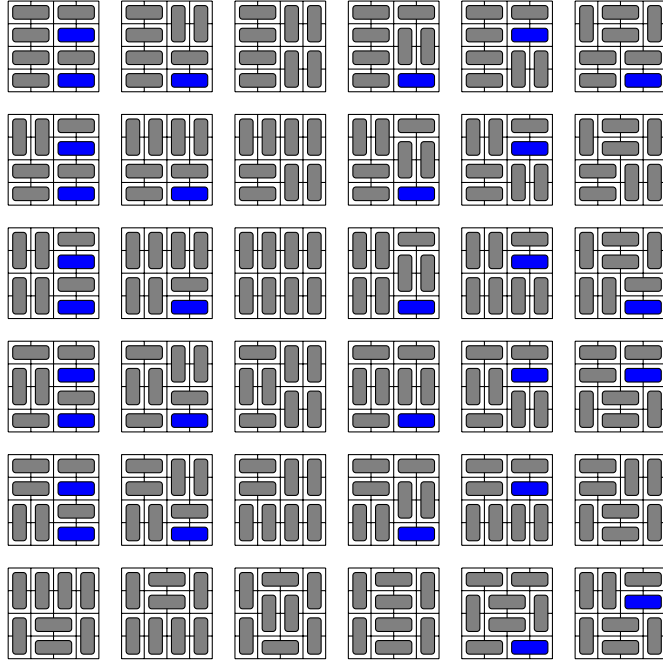


FIGURE 8. The 36 domino tilings of a 4×4 checkerboard. The blue dominos are assigned weight 2 for the purposes of Theorem 4.5.

Part (4) of the following theorem is the well-known formula due to Kasteleyn [18] and to Temperley and Fisher [39] for the number of domino tilings of a checkerboard. We provide a new proof.

Theorem 4.2. *Let $U_j(x)$ denote the j -th Chebyshev polynomial of the second kind, and let*

$$\xi_{h,d} := \cos\left(\frac{h\pi}{2d+1}\right),$$

for all integers h and d . Then for all integers $m, n \geq 1$, the following are equal:

- (1) the number of symmetric recurrents on $\text{SF}_{2m \times 2n}$;
- (2) the number of domino tilings of a $2m \times 2n$ checkerboard;
- (3)

$$(-1)^{mn} \prod_{h=1}^m U_{2n}(\xi_{h,m});$$

(4)

$$\prod_{h=1}^m \prod_{k=1}^n (4\xi_{h,m}^2 + 4\xi_{k,n}^2).$$

Proof. It may be helpful to read Example 4.4 in parallel with this proof.

Let $A_n = (a_{h,k})$ be the $n \times n$ tridiagonal matrix with entries

$$a_{h,k} = \begin{cases} 4 & \text{if } h = k \neq n, \\ 3 & \text{if } h = k = n, \\ -1 & \text{if } |h - k| = 1, \\ 0 & \text{if } |h - k| \geq 2. \end{cases}$$

In particular, $A_1 = [3]$. Take the vertices $[m] \times [n]$ as representatives for the orbits of G acting on the non-sink vertices of $\text{SF}_{2m \times 2n}$. Ordering these representatives lexicographically, i.e., left-to-right then top-to-bottom, the symmetrized reduced Laplacian (2.2) is given by the $mn \times mn$ tridiagonal block matrix

$$(4.9) \quad \tilde{\Delta}^G = \begin{bmatrix} A_n & -I_n & & \cdots & & 0 \\ -I_n & A_n & -I_n & & & \\ & \ddots & \ddots & \ddots & & \vdots \\ & & -I_n & A_n & -I_n & \\ \vdots & & & \ddots & \ddots & \ddots \\ & & & & -I_n & A_n & -I_n \\ 0 & \cdots & & & -I_n & B_n \end{bmatrix}$$

where I_n is the $n \times n$ identity matrix and $B_n := A_n - I_n$. If $m = 1$, then $\tilde{\Delta}^G := B_n$.

[(1) = (2)]: The matrix $\tilde{\Delta}^G$ is the reduced Laplacian of a sandpile graph we now describe. Let $D_{m \times n}$ be the graph obtained from $\Gamma_{m \times n}$, the ordinary grid graph, by adding (i) a sink vertex, s' , (ii) an edge of weight 2 from the vertex $(1, 1)$ to s' , and (iii) edges of weight 1 from each of the other vertices along the left and top sides to s' , i.e., $\{(h, 1), s'\}$ for $1 < h \leq m$ and $\{(1, k), s'\}$ for $1 < k \leq n$. We embed $D_{m \times n}$ in the plane so that the non-sink vertices form an ordinary grid, and the

edge of weight 2 is represented by a pair of edges of weight 1, forming a digon. Then, $\mathcal{H}(D_{m \times n}) = \Gamma_{2m \times 2n}$ (see Figure 11).

Since $\tilde{\Delta}^G = \tilde{\Delta}_{D_{m \times n}}$, taking determinants shows that the number of symmetric recurrents on $\text{S}\Gamma_{2m \times 2n}$ is equal to the size of the sandpile group of $D_{m \times n}$, and hence to the number of spanning trees of $D_{m \times n}$ rooted at s' , counted according to weight. These spanning trees are, in turn, in bijection with the perfect matchings of the graph $\mathcal{H}(D_{m \times n}) = \Gamma_{2m \times 2n}$ obtained from the generalized Temperley bijection of Section 3. Hence, the numbers in parts (1) and (2) are equal.

[(1) = (3)]: By Corollary 2.11, $\det \tilde{\Delta}^G$ is the number of symmetric recurrents on $\text{S}\Gamma_{2m \times 2n}$. By Lemma 4.1,

$$(4.10) \quad \det \tilde{\Delta}^G = (-1)^n \det(T),$$

where

$$\begin{aligned} T &= -B_n U_{m-1} \left(\frac{A_n}{2} \right) + U_{m-2} \left(\frac{A_n}{2} \right) \\ &= -(A_n - I_n) U_{m-1} \left(\frac{A_n}{2} \right) + U_{m-2} \left(\frac{A_n}{2} \right) \\ &= U_{m-1} \left(\frac{A_n}{2} \right) - \left(A_n U_{m-1} \left(\frac{A_n}{2} \right) - U_{m-2} \left(\frac{A_n}{2} \right) \right) \\ &= U_{m-1} \left(\frac{A_n}{2} \right) - U_m \left(\frac{A_n}{2} \right). \end{aligned}$$

Using (4.4) and the fact that the Chebyshev polynomials of the second kind satisfy

$$U_j(\cos \theta) = \frac{\sin((j+1)\theta)}{\sin \theta},$$

it is easy to check that the polynomial

$$p(x) := U_m \left(\frac{x}{2} \right) - U_{m-1} \left(\frac{x}{2} \right)$$

is a monic polynomial of degree m with zeros

$$t_{h,m} := 2 \cos \frac{(2h+1)\pi}{2m+1}, \quad 0 \leq h \leq m-1.$$

Thus,

$$T = -p(A_n) = - \prod_{h=0}^{m-1} (A_n - t_{h,m} I_n),$$

and by equation (4.10),

$$\det \tilde{\Delta}^G = \prod_{h=0}^{m-1} \chi_n(t_{h,m}),$$

where $\chi_n(x)$ is the characteristic polynomial of A_n . Therefore, to show that the expressions in parts (1) and (3) are equal, it suffices to show that

$$(4.11) \quad \chi_n(t_{h,m}) = (-1)^n U_{2n}(i \xi_{m-h,m})$$

for each $h \in \{0, 1, \dots, m-1\}$, which we do by showing that both sides of the equation satisfy the same recurrence.

Define $\chi_0(x) := 1$. Expanding the determinant defining $\chi_n(x)$, starting along the first row, leads to a recursive formula for $\chi_n(x)$:

$$(4.12) \quad \begin{aligned} \chi_0(x) &= 1 \\ \chi_1(x) &= 3 - x \\ \chi_j(x) &= (4 - x)\chi_{j-1}(x) - \chi_{j-2}(x) \quad \text{for } j \geq 2. \end{aligned}$$

On the other hand, defining $C_j(x) := (-1)^j U_{2j}(x)$, it follows from (4.2) that

$$(4.13) \quad \begin{aligned} C_0(x) &= 1 \\ C_1(x) &= 1 - 4x^2 \\ C_j(x) &= (2 - 4x^2)C_{j-1}(x) - C_{j-2}(x) \quad \text{for } j \geq 2. \end{aligned}$$

The result now follows by letting $x = t_{h,m}$ in (4.12), letting $x = i \xi_{m-h,m}$ in (4.13), and using the fact that

$$(4.14) \quad t_{h,m} = 2 - 4 \xi_{m-h,m}^2.$$

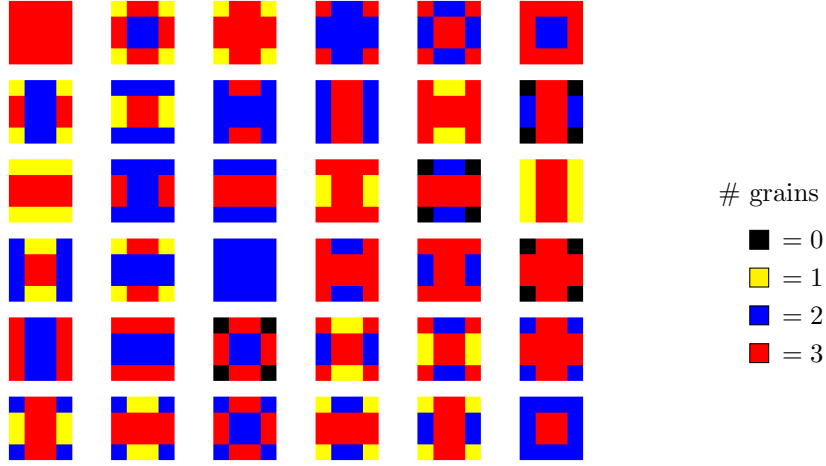
(Equation (4.14) can be verified using, for example, the double-angle formula for cosine and the relation among angles, $(2h+1)\pi/(2m+1) = \pi - 2(m-h)\pi/(2m+1)$).

[(3) = (4)]: Using (4.4),

$$\begin{aligned} & (-1)^{mn} \prod_{h=1}^m U_{2n}(i \xi_{h,m}) \\ &= (-1)^{mn} \prod_{h=1}^m \prod_{k=1}^{2n} (2i \xi_{h,m} - 2 \xi_{k,n}) \\ &= (-1)^{mn} \prod_{h=1}^m \prod_{k=1}^n (2i \xi_{h,m} - 2 \xi_{k,n})(2i \xi_{h,m} + 2 \xi_{k,n}) \\ &= \prod_{h=1}^m \prod_{k=1}^n (4 \xi_{h,m}^2 + 4 \xi_{k,n}^2). \end{aligned}$$

□

Example 4.3. Figure 9 lists the 36 symmetric recurrents on $\text{SF}_{4 \times 4}$ in no particular order. Given a symmetric recurrent, c , let \tilde{c} be the restriction of c to the vertices $(1,1)$, $(1,2)$, $(2,1)$, and $(2,2)$, representing the orbits of the Klein 4-group action on $\text{SF}_{4 \times 4}$. We regard \tilde{c} as a configuration on $D_{2 \times 2}$, the sandpile graph introduced in the proof of Theorem 4.2. Let $\iota(c)$ be the recurrent element of the sandpile graph $D_{2 \times 2}$ equivalent to \tilde{c} modulo the reduced Laplacian of $D_{2 \times 2}$. Then $c \mapsto \iota(c)$ determines a bijection between the symmetric recurrents of $\text{SF}_{4 \times 4}$ and the recurrents of $D_{2 \times 2}$. In [14], it is shown that the sandpile group of a graph acts freely and transitively on the set of spanning trees of the graph rooted at the sink, i.e., this set of spanning trees is a *torsor* for the sandpile group. Thus, via the Temperley bijection, the domino tilings of the 4×4 checkerboard, forms a torsor for the group of symmetric recurrents on $\text{SF}_{4 \times 4}$. □

FIGURE 9. The 36 symmetric recurrents on $\text{SF}_{4 \times 4}$.

Example 4.4. This example illustrates part of the proof of Theorem 4.2 for the case $m = 4$ and $n = 3$. Figure 10 shows the graph $\text{SF}_{8 \times 6}$. The boxed 4×3 block of vertices in the upper left are representatives of the orbits of the Klein 4-group action. Order these from left-to-right, top-to-bottom, to get the matrix for the symmetrized reduced Laplacian, $\tilde{\Delta}_{8 \times 6}^G$. The vertex $(2, 3)$ of SF_8 in Figure 10 is colored blue. If this vertex is fired simultaneously with the other vertices in its orbit, it will lose 4 grains of sand to its neighbors but gain 1 grain of sand from the adjacent vertex in its orbit. This firing-rule is encoded in the sixth column of $\tilde{\Delta}_{8 \times 6}^G$ (shaded blue).

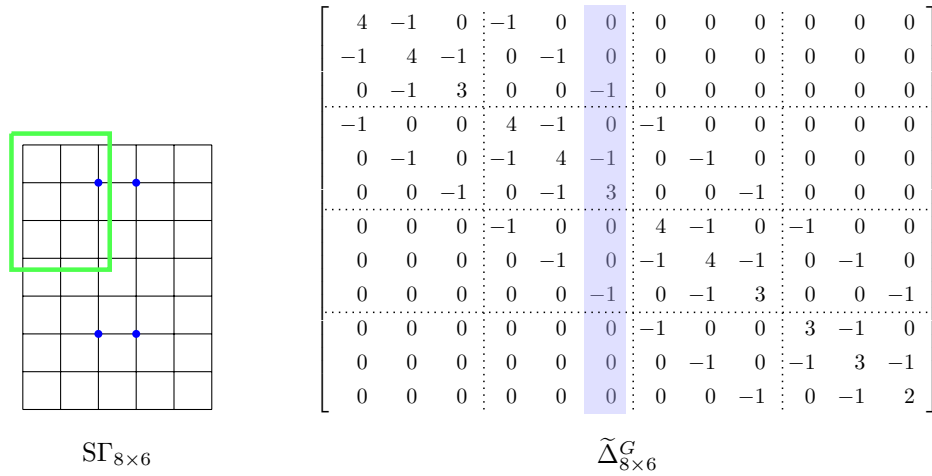


FIGURE 10. A sandpile grid graph and its symmetrized reduced Laplacian.

The matrix $\tilde{\Delta}_{8 \times 6}^G$ is the reduced Laplacian of the graph $D_{4 \times 3}$, shown in Figure 11. To form $\mathcal{H}(D_{4 \times 3}) = \Gamma_{8 \times 6}$, we first overlay $D_{4 \times 3}$ with its dual, as shown, then remove the vertices s and \tilde{s} and their incident edges. Figure 12 shows how a spanning tree of $D_{4 \times 3}$ (in black) determines a spanning tree of the dual graph (in blue) and a domino tiling of the 8×6 checkerboard.

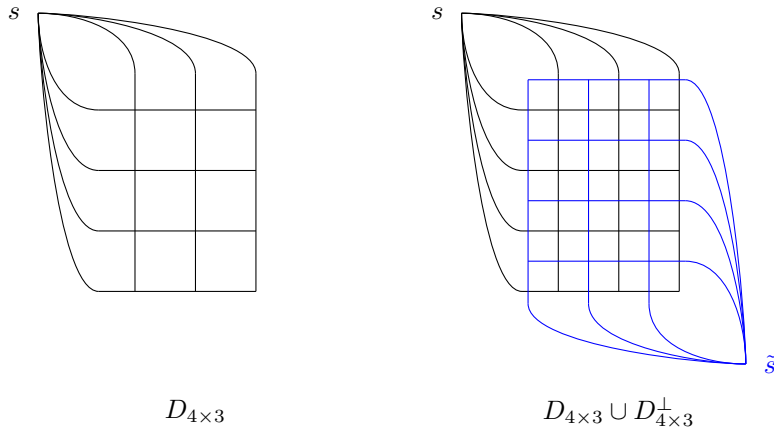


FIGURE 11. The symmetrized reduced Laplacian for $S\Gamma_{8 \times 6}$ is the reduced Laplacian for $D_{4 \times 3}$. Removing s and \tilde{s} and their incident edges from the graph on the right shows $\mathcal{H}(D_{4 \times 3}) = \Gamma_{8 \times 6}$.

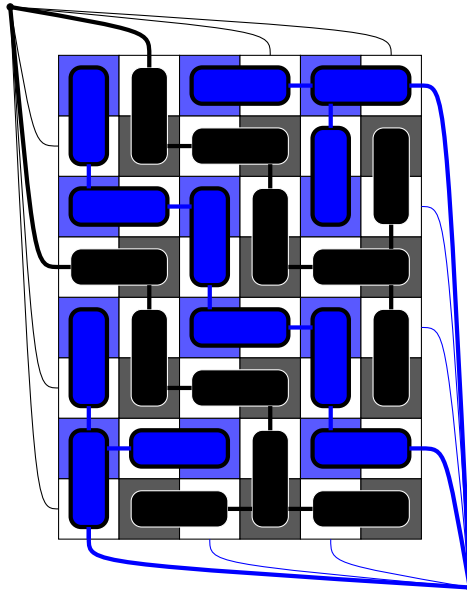


FIGURE 12. Every domino tiling of an even-sided checkerboard consists of a spanning tree entwined with its dual spanning tree.

□

4.3. Symmetric recurrences on a $2m \times (2n - 1)$ sandpile grid graph. The $m \times n$ Möbius grid graph, $\Gamma_{m \times n}^{\text{mob}}$, is the graph formed from the ordinary $m \times n$ grid graph, $\Gamma_{m \times n}$, by adding the edges $\{(h, 1), (m - h + 1, n)\}$ for $1 \leq h \leq m$. A Möbius checkerboard is an ordinary checkerboard with its left and right sides glued with a twist. Domino tilings of an $m \times n$ Möbius checkerboard are identified with perfect matchings of $\Gamma_{m \times n}^{\text{mob}}$. See Figure 13 for examples.

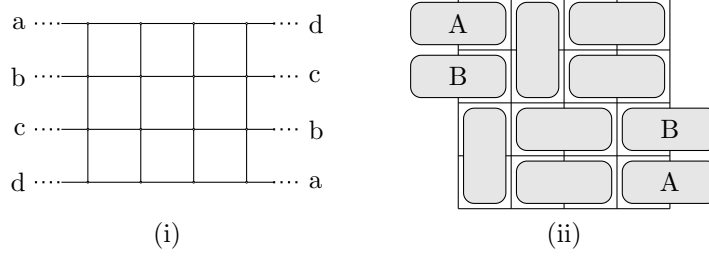


FIGURE 13. (i) The 4×4 Möbius grid graph, $\Gamma_{4 \times 4}^{\text{mob}}$; (ii) A tiling of the 4×4 Möbius checkerboard.

As part of Theorem 4.5, we will show that the domino tilings of a $2m \times 2n$ Möbius checkerboard can be counted using weighted domino tilings of an associated ordinary checkerboard, which we now describe. Define the Möbius-weighted $m \times n$ grid graph, $M\Gamma_{m \times n}$, as the ordinary $m \times n$ grid graph but with each edge of the form $\{(m - 2h, n - 1), (m - 2h, n)\}$ for $0 \leq h < \lfloor \frac{m}{2} \rfloor$ assigned the weight 2, and, if m is odd, then in addition assign the edge $\{(1, n - 1), (1, n)\}$ the weight 3 (and all other edges have weight 1). (In the case $m = 1$, the weight of the edge $\{(1, n - 1), (1, n)\}$ is defined to be 3.) See Figure 14 for examples. The Möbius-weighted $m \times n$

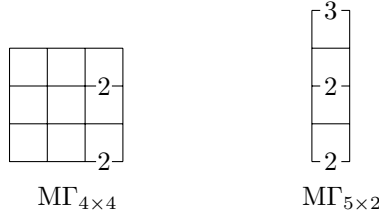


FIGURE 14. Two Möbius-weighted grid graphs.

checkerboard is the ordinary $m \times n$ checkerboard but for which the weight of a domino tiling is taken to be the weight of the corresponding perfect matching of $M\Gamma_{m \times n}$. In Figure 8, the dominos corresponding to edges of weight 2 are shaded. Thus, the first three tilings in the first row of Figure 8 have weights 4, 2, and 1, respectively. Example 4.9 considers a case for which m is odd.

Theorem 4.5. Let $T_j(x)$ denote the j -th Chebyshev polynomial of the first kind, and let

$$\xi_{h,d} := \cos\left(\frac{h\pi}{2d+1}\right) \quad \text{and} \quad \zeta_{h,d} := \cos\left(\frac{(2h-1)\pi}{4d}\right)$$

for all integers h and $d \neq 0$. Then for all integers $m, n \geq 1$, the following are equal:

- (1) the number of symmetric recurrents on $\text{S}\Gamma_{2m \times (2n-1)}$;
(2) if $n > 1$, the number of domino tilings of the Möbius-weighted $2m \times 2n$ checkerboard, and if $n = 1$, the number of domino tilings of the Möbius-weighted $(2m - 1) \times 2$ checkerboard, counted according to weight;
(3)

$$(-1)^{mn} 2^m \prod_{h=1}^m T_{2n}(i \xi_{h,m});$$

(4)

$$\prod_{h=1}^m \prod_{k=1}^n (4 \xi_{h,m}^2 + 4 \xi_{k,n}^2);$$

- (5) the number of domino tilings of a $2m \times 2n$ Möbius checkerboard.

Remark 4.6. By identity (4.5),

$$T_{2n}(i \xi_{h,m}) = (-1)^n T_n(1 + 2 \xi_{h,m}^2),$$

from which it follows, after proving Theorem 4.5, that

$$2^m \prod_{h=1}^m T_n(1 + 2 \xi_{h,m}^2)$$

is another way to express the numbers in parts (1)–(5).

Proof of Theorem 4.5. The proof is similar to that of Theorem 4.2 after altering the definitions of the matrices A_n and B_n used there. This time, for $n > 1$, let $A'_n = (a'_{h,k})$ be the $n \times n$ tridiagonal matrix with entries

$$a'_{h,k} = \begin{cases} 4 & \text{if } h = k, \\ -1 & \text{if } |h - k| = 1 \text{ and } h \neq n, \\ -2 & \text{if } h = n \text{ and } k = n - 1, \\ 0 & \text{if } |h - k| \geq 2. \end{cases}$$

In particular, $A'_1 = [4]$. Define the matrix $B'_n = (b'_{h,k})$ by

$$b'_{h,k} = \begin{cases} 3 & \text{if } h = k, \\ a'_{h,k} & \text{otherwise.} \end{cases}$$

Thus, for instance,

$$A'_3 = \begin{bmatrix} 4 & -1 & 0 \\ -1 & 4 & -1 \\ 0 & -2 & 4 \end{bmatrix}, \quad B'_3 = \begin{bmatrix} 3 & -1 & 0 \\ -1 & 3 & -1 \\ 0 & -2 & 3 \end{bmatrix}.$$

If $n = 1$, take $A'_1 = [4]$ and $B'_1 = [3]$.

(1) = (2): Reasoning as in the proof of Theorem 4.2, equation (4.9) with A'_n and B'_n substituted for A_n and B_n gives the symmetrized reduced Laplacian, $\tilde{\Delta}^G$, of $\text{S}\Gamma_{2m \times (2n-1)}$. Unless $n = 1$, the matrix $\tilde{\Delta}^G$ is *not* the reduced Laplacian matrix of a sandpile graph since the sum of the elements in its penultimate column is -1 whereas the sum of the elements in any column of the reduced Laplacian of a sandpile graph must be nonnegative. However, in any case, the transpose $(\tilde{\Delta}^G)^t$ is the reduced Laplacian of a sandpile graph, which we call $D'_{m \times n}$. We embed it in

the plane as a grid as we did previously with $D_{m \times n}$ in the proof of Theorem 4.2, but this time with some edge-weights not equal to 1.

Figure 15 shows $D'_{4 \times 3}$. It is the same as $D_{4 \times 3}$ as depicted in Figure 11, except that arrowed edges, \longleftrightarrow , have been substituted for certain edges. Each represents a pair of arrows—one from right-to-left of weight 2 and one from left-to-right of weight 1—embedded so that they coincide, as discussed in Section 3.

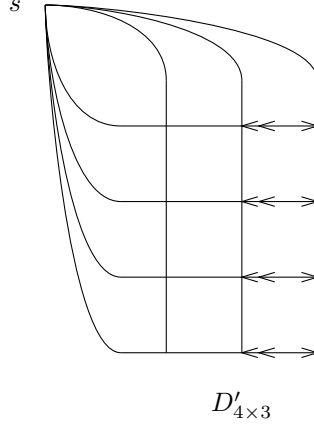


FIGURE 15. The symmetrized reduced Laplacian for $\text{SG}_{8 \times 5}$ is the reduced Laplacian for $D'_{4 \times 3}$. Arrowed edges each represent a pair of directed edges of weights 1 and 2, respectively, as indicated by the number of arrow heads. All other edges have weight 1.

Reasoning as in the proof of Theorem 4.2, we see that the number of perfect matchings of $\mathcal{H}(D'_{m \times n})$ is equal to the number of perfect matchings of $\text{MG}_{2m \times (2n-1)}$, each counted according to weight. This number is $\det(\tilde{\Delta}^G)^t = \det \tilde{\Delta}^G$, which is the number of symmetric recurrents on $\text{SG}_{2m \times (2n-1)}$ by Corollary 2.11.

[(1) = (3)]: Exactly the same argument as given in the proof of Theorem 4.2 shows that

$$\det \tilde{\Delta}^G = \prod_{h=0}^{m-1} \chi_n(t_{h,m}),$$

where $t_{h,m}$ is as before, but now $\chi_n(x)$ is the characteristic polynomial of A'_n . In light of Remark 4.6, it suffices to show

$$\chi_n(t_{h,m}) = 2T_n(1 + 2\xi_{m-h,m}^2)$$

for each $h \in \{0, 1, \dots, m-1\}$, which we now do as before, by showing both sides of the equation satisfy the same recurrence.

Defining $\chi_0(x) := 2$ and expanding the determinant defining $\chi_n(x)$ yields

$$(4.15) \quad \begin{aligned} \chi_0(x) &= 2 \\ \chi_1(x) &= 4 - x \\ \chi_j(x) &= (4 - x)\chi_{j-1}(x) - \chi_{j-2}(x) \quad \text{for } j \geq 2. \end{aligned}$$

On the other hand, defining $C_j(x) := 2T_j(x)$, it follows from (4.1) that

$$(4.16) \quad \begin{aligned} C_0(x) &= 2 \\ C_1(x) &= 2x \\ C_j(x) &= 2x C_{j-1}(x) - C_{j-2}(x) \quad \text{for } j \geq 2. \end{aligned}$$

The result now follows as before, using equation (4.14).

[(3) = (4)]: The numbers given in parts (3) and (4) are equal by a straightforward calculation, similar to that in the proof of the analogous result in Theorem 4.2, this time using (4.3).

[(4) = (5)]: Formula (2) in [21] gives the number of domino tilings of a $2m \times 2n$ Möbius checkerboard. That formula is identical to our double-product in part (4) but with $\sin((4k-1)\pi/(4n))$ substituted for $\zeta_{k,n}$. Now,

$$\sin\left(\frac{(4k-1)\pi}{4n}\right) = \cos\left(\frac{(4k-1-2n)\pi}{4n}\right).$$

Defining $\theta(k) = (2k-1)\pi/(4n)$ and $\psi(k) = (4k-1-2n)\pi/(4n)$, it therefore suffices to show that there is a permutation σ of $\{1, \dots, n\}$ such that $\theta(k) = \pm\psi(\sigma(k))$ for $k = 1, \dots, n$ because, in that case, $\zeta_{k,n} = \cos(\theta(k)) = \cos(\psi(\sigma(k)))$. Such a permutation exists, for if $n = 2t$, then

$$\begin{aligned} \theta(2\ell-1) &= -\psi(t-\ell+1), & 1 \leq \ell \leq t, \\ \theta(2\ell) &= \psi(\ell+t), & 1 \leq \ell \leq t, \end{aligned}$$

and if $n = 2t-1$, then

$$\begin{aligned} \theta(2\ell-1) &= \psi(t+\ell-1), & 1 \leq \ell \leq t, \\ \theta(2\ell) &= -\psi(t-\ell), & 1 \leq \ell \leq t-1. \end{aligned}$$

□

Remark 4.7. In the proof of Theorem 4.5, we rewrote the double-product in part (4) as the Lu-Wu formula ((2) in [21]) for the number of domino tilings of the $2m \times 2n$ Möbius checkerboard:

$$\prod_{h=1}^m \prod_{k=1}^n (4\xi_{h,m}^2 + 4\mu_{k,n}^2),$$

where $\mu_{k,n} := \sin((4k-1)\pi/(4n))$. Thus, it is the work of Lu and Wu that allowed us to add part (5) to Theorem 4.5. This is in contrast to Theorem 4.2, which gave an independent proof of the Kastelyn and Temperley-Fisher formula for the number of tilings of the ordinary $2m \times 2n$ checkerboard.

Example 4.8. The 36 tilings of the ordinary 4×4 checkerboard are listed in Figure 8. Considering these as tilings of the Möbius-weighted 4×4 checkerboard, the sum of the weights of the tilings is 71, which is the number of tilings of the 4×4 Möbius checkerboard and the number of symmetric recurrences on $\text{SG}_{4 \times 3}$, in accordance with Theorem 4.5. □

Example 4.9. Figure 16 shows the domino tilings of the Möbius-weighted 5×2 checkerboard. The total number of tilings, counted according to weight, is 41, which is the number of domino tilings of a 6×2 Möbius checkerboard, in agreement with case $m = 3$ and $n = 1$ of Theorem 4.5. □

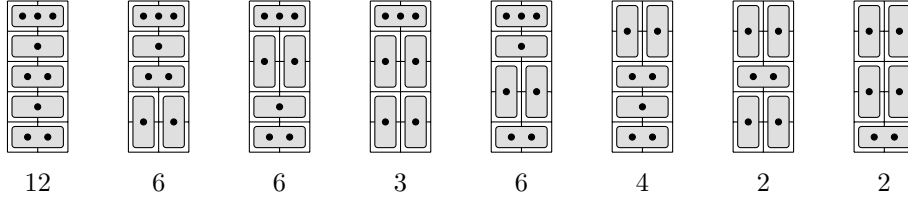


FIGURE 16. Domino tilings of the Möbius-weighted 5×2 checkerboard. The number of dots on each domino indicates its weight. The weight of each tiling appears underneath.

4.4. Symmetric recurrences on a $(2m - 1) \times (2n - 1)$ sandpile grid graph.

The *2-weighted* $2m \times 2n$ grid graph, $2\text{-}\Gamma_{2m \times 2n}$ is the ordinary $2m \times 2n$ grid graph but where each horizontal edge of the form $\{(2m - 2h, 2n - 1), (2m - 2h, 2n)\}$ for $0 \leq h < m$ and each vertical edge of the form $\{(2m - 1, 2n - 2k), (2m, 2n - 2k)\}$ for $0 \leq k < n$ is assigned the weight 2 (and all other edges have weight 1). See Figure 14 for an example. The *2-weighted* $2m \times 2n$ checkerboard is the ordinary $2m \times 2n$ checkerboard but for which the weight of a domino tiling is taken to be the weight of the corresponding perfect matching of $2\text{-}\Gamma_{2m \times 2n}$.

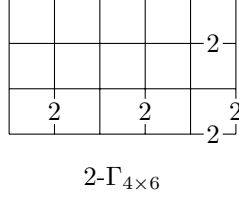


FIGURE 17. A 2-weighted grid graph.

Theorem 4.10. Let $T_j(x)$ denote the j -th Chebyshev polynomial of the first kind, and let

$$\zeta_{h,d} := \cos\left(\frac{(2h-1)\pi}{4d}\right)$$

for all integers h and $d \neq 0$. Then for all integers $m, n \geq 1$, the following are equal:

- (1) the number of symmetric recurrences on $\text{SI}\Gamma_{(2m-1) \times (2n-1)}$;
- (2) the number of domino tilings of the 2-weighted checkerboard of size $2m \times 2n$;
- (3)

$$(-1)^{mn} 2^m \prod_{h=1}^m T_{2n}(i\zeta_{h,m});$$

- (4)

$$\prod_{h=1}^m \prod_{k=1}^n (4\zeta_{h,m}^2 + 4\zeta_{k,n}^2).$$

Remark 4.11. As in Remark 4.6, we use identity (4.5), this time to get

$$T_{2n}(i\zeta_{h,m}) = (-1)^n T_n(1 + 2\zeta_{h,m}^2),$$

allowing us to equate the formula in part (3) with

$$2^m \prod_{h=1}^m T_n(1 + 2\zeta_{h,m}^2).$$

(We do not know of an analogous expression for the formula in Theorem 4.2 (3) in terms of products of n -th Chebyshev polynomials.)

Proof. The proof is similar to those for Theorem 4.2 and Theorem 4.5. Let A'_n be the matrix defined at the beginning of the proof of Theorem 4.5. Then the symmetrized reduced Laplacian, $\tilde{\Delta}^G$, for $2\text{-}\Gamma_{(2m-1)\times(2n-1)}$ is the matrix $D(m)$ displayed in the statement of Lemma 4.1 after setting $A = B = A'_n$ and $C = 2I_n$.

[(1) = (2)]: The transpose $(\tilde{\Delta}^G)^t$ is the reduced Laplacian of a sandpile graph, which we denote by $D''_{m\times n}$ and embed in the plane as we did previously for $D_{m\times n}$ and $D'_{m\times n}$ in Theorems 4.2 and 4.5. The embedding of $D''_{m\times n}$ differs from that of $D'_{m\times n}$ only in that each edge of the form $((m, i), (m-1, i))$ where $i \in [n]$ now carries weight 2, again embedded as one edge coincident with the edge $((m-1, i), (m, i))$ in the plane (Figure 18 displays $D''_{4\times 3}$). The result for this section of the proof now

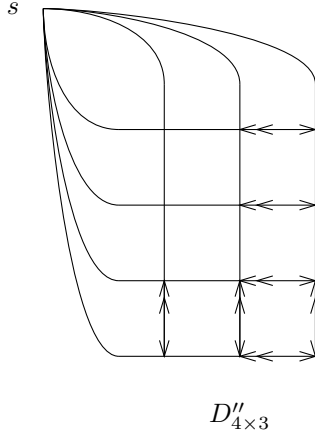


FIGURE 18. The symmetrized reduced Laplacian for $S\Gamma_{7\times 5}$ is the reduced Laplacian for $D''_{4\times 3}$. (The edge weights are encoded as in Figure 15).

follows just as it did in the proof of Theorem 4.5.

[(1) = (3)]: By Corollary 2.11 and Lemma 4.1, the number of symmetric recurrents on $2\text{-}\Gamma_{(2m-1)\times(2n-1)}$ is

$$\det \tilde{\Delta}^G = (-1)^n \det(T),$$

where

$$T = -A'_n U_{m-1} \begin{pmatrix} A'_n \\ 2 \end{pmatrix} + 2U_{m-2} \begin{pmatrix} A'_n \\ 2 \end{pmatrix}.$$

Define

$$s_{h,m} := \cos \frac{(2h-1)\pi}{2m}, \quad 1 \leq h \leq m.$$

Then, using identities from Section 4.1,

$$\begin{aligned} T &= -U_m \left(\frac{A'_n}{2} \right) + U_{m-2} \left(\frac{A'_n}{2} \right) \\ &= -2T_m \left(\frac{A'_n}{2} \right) \\ &= -\prod_{h=1}^m (A'_n - 2s_{h,m}I_n), \end{aligned}$$

Thus,

$$\det \tilde{\Delta}^G = \prod_{h=1}^m \chi_n(2s_{h,m}),$$

where χ_n is the characteristic polynomial of A'_n . Now consider the recurrences (4.15) and (4.16) in the proof of Theorem 4.5. Substituting $2s_{h,m}$ for x in the former and $2 - s_{h,m}$ for x in the latter, the two recurrences become the same. It follows that $\chi_n(2s_{h,m}) = 2T_n(2 - s_{h,m})$. Then using a double-angle formula for cosine and identity (4.5),

$$\chi_n(2s_{h,m}) = 2T_n(2 - s_{h,m}) = 2T_n(1 + 2\zeta_{m-h+1,m}^2),$$

and the result follows from Remark 4.11.

[(3) = (4)]: The numbers given in parts (3) and (4) are equal by a straightforward calculation, as in the proof of the analogous results in Theorems 4.2 and 4.5. \square

Remark 4.12. Identities among trigonometric functions and among Chebyshev polynomials allow our formulae to be recast many ways. Remarks 4.6, 4.7, and 4.11 have already provided some examples. In addition, we note that in part (4) of Theorem 4.5 and in parts (3) and (4) of Theorem 4.10, one may replace each $\zeta_{h,n}$ with $\sin((2h-1)\pi/(4n))$ or, as discussed at the end of the proof of Theorem 4.5, with $\sin((4h-1)\pi/(4n))$.

5. THE ORDER OF THE ALL-TWOS CONFIGURATION

Let c be a configuration on a sandpile graph Γ , not necessarily an element of $\mathcal{S}(\Gamma)$, the sandpile group. If k is a nonnegative integer, let $k \cdot c$ denote the vertex-wise addition of c with itself k times, without stabilizing. The *order* of c , denoted $\text{order}(c)$, is the smallest positive integer k such that $k \cdot c$ is in the image of the reduced Laplacian of Γ . If c is recurrent, then the order of c is the same as its order as an element of $\mathcal{S}(\Gamma)$ according to the isomorphism (2.1).

Consider the sandpile grid graph, $\text{S}\Gamma_{m \times n}$, with $m, n \geq 2$. For each nonnegative integer k , let $\vec{k}_{m \times n} = k \cdot \vec{1}_{m \times n}$ be the *all- k s* configuration on $\text{S}\Gamma_{m \times n}$ consisting of k grains of sand on each vertex. The motivating question for this section is: what is the order of $\vec{1}_{m \times n}$? Since $\vec{1}_{m \times n}$ has up-down and left-right symmetry, its order must divide the order of the group of symmetric recurrents on $\text{S}\Gamma_{m \times n}$ calculated in Theorems 4.2, 4.5, and 4.10. The number of domino tilings of a $2n \times 2n$ checkerboard can be written as $2^n a_n^2$ where a_n is an odd integer (cf. Proposition 5.3). Our main result is Theorem 5.5 which, through Corollary 5.6, says that the order of $\vec{2}_{2n \times 2n}$ divides a_n .

Proposition 5.1. *Let $m, n \geq 2$.*

- (1) The configuration $\vec{1}_{m \times n}$ is not recurrent.
- (2) The configuration $\vec{2}_{m \times n}$ is recurrent.
- (3) The order of $\vec{1}_{m \times n}$ is either $\text{order}(\vec{2}_{m \times n})$ or $2 \text{order}(\vec{2}_{m \times n})$.
- (4) Let $\tilde{\Delta}_{m \times n}$ be the reduced Laplacian of $\text{S}\Gamma_{m \times n}$. The order of $\vec{1}_{m \times n}$ is the smallest integer k such that $k \cdot \tilde{\Delta}_{m \times n}^{-1} \vec{1}_{m \times n}$ is an integer vector.

Proof. Part (1) follows immediately from the burning algorithm (Theorem 2.1). For part (2), we start by orienting some of the edges of $\text{S}\Gamma_{m \times n}$ as shown in Figure 19. First, orient all the edges containing the sink, s , so that they point away from s .

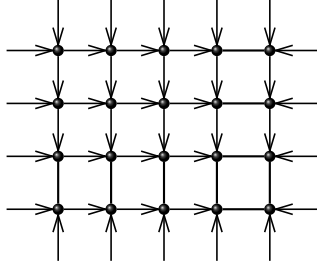


FIGURE 19. Partial orientation of $\text{S}\Gamma_{4 \times 5}$. Arrows pointing into the grid from the outside represent edges from the sink vertex.

Next, orient all the horizontal edges to point to the right except for the last column of horizontal arrows. Finally, orient all the vertical edges down except for the last row of vertical arrows. More formally, define the *partial orientation* of $\text{S}\Gamma_{m \times n}$,

$$\begin{aligned} \mathcal{O} := & \{(s, (i, j)) : 1 \leq i \leq m, j \in \{1, n\}\} \\ & \cup \{(s, (i, j)) : i \in \{1, m\}, 1 \leq j \leq n\} \\ & \cup \{((i, j), (i, j+1)) : 1 \leq j \leq n-2\} \\ & \cup \{((i, j), (i+1, j)) : 1 \leq i \leq m-2\}. \end{aligned}$$

Use \mathcal{O} to define a poset P on the vertices of $\text{S}\Gamma_{m \times n}$ by first setting $u <_P v$ if $(u, v) \in \mathcal{O}$, then taking the transitive closure. Now list the vertices of $\text{S}\Gamma_{m \times n}$ in any order v_1, v_2, \dots such that $v_i <_P v_j$ implies $i < j$. Thus, $v_1 = s$ and v_2, v_3, v_4, v_5 are the four corners of the grid, in some order. Starting from $\vec{2}_{m \times n}$, fire v_1 . This has the effect of adding the burning configuration to $\vec{2}_{m \times n}$. Since the indegree of each non-sink vertex with respect to \mathcal{O} is 2, after v_1, \dots, v_{i-1} have fired, v_i is unstable. Thus, after firing the sink, every vertex will fire while stabilizing the resulting configuration. So $\vec{2}_{m \times n}$ is recurrent by the burning algorithm.

[NOTE: One way to think about listing the vertices, as prescribed above, is as follows. Let $P_{-1} := \{s\}$, and for $i \geq 0$, let P_i be those elements whose distance from some corner vertex is i . (By *distance* from a corner vertex, we mean the length of a longest chain in P or the length of any path in \mathcal{O} starting from a corner vertex.) For instance, P_0 consists of the four corners. After firing the vertices in $P_{-1}, P_0, \dots, P_{i-1}$, all of the vertices in P_i are unstable and can be fired in any order.]

For part (3), let $\alpha = \text{order}(\vec{1}_{m \times n})$ and $\beta = \text{order}(\vec{2}_{m \times n})$, and let e be the identity of $\mathcal{S}(\text{S}\Gamma_{m \times n})$. Let $\tilde{\mathcal{L}}$ denote the image of the reduced Laplacian, $\tilde{\Delta}$, of $\text{S}\Gamma_{m \times n}$. Since

$e = (2\alpha \cdot \vec{1}_{m \times n})^\circ = (\alpha \cdot \vec{2}_{m \times n})^\circ$ and $e = (\beta \cdot \vec{2}_{m \times n})^\circ = (2\beta \cdot \vec{1}_{m \times n})^\circ$, we have

$$(5.1) \quad 2\beta \geq \alpha \geq \beta.$$

We have $(2\beta - \alpha) \cdot \vec{1}_{m \times n} = 0 \pmod{\tilde{\mathcal{L}}}$. Suppose $\alpha \neq 2\beta$. It cannot be that $2\beta - \alpha = 1$. Otherwise, $\vec{1}_{m \times n} = 0 \pmod{\tilde{\mathcal{L}}}$. It would then follow that $\vec{2}_{m \times n}$ and $\vec{3}_{m \times n}$ are recurrent elements equivalent to 0 modulo $\tilde{\mathcal{L}}$, whence, $\vec{2}_{m \times n} = \vec{3}_{m \times n} = e$, a contradiction. Thus, $(2\beta - \alpha) \cdot \vec{1}_{m \times n} \geq \vec{2}_{m \times n}$. Since $\vec{2}_{m \times n}$ is recurrent, $((2\beta - \alpha) \cdot \vec{1}_{m \times n})^\circ$ is recurrent and equivalent to 0 modulo $\tilde{\mathcal{L}}$, and thus must be the e . So $2\beta - \alpha \geq \alpha$, and the right side of (5.1) implies $\alpha = \beta$, as required.

Now consider part (4). The order of $\vec{1}_{m \times n}$ is the smallest positive integer k such that $k \cdot \vec{1}_{m \times n} = 0 \pmod{\tilde{\mathcal{L}}}$, i.e., for which there exists an integer vector v such that $k \cdot \vec{1}_{m \times n} = \vec{\Delta}_{m \times n} v$. The result follows. \square

Example 5.2. We have $\text{order}(\vec{1}_{2 \times 2}) = 2 \text{order}(\vec{2}_{2 \times 2}) = 2$, and $\text{order}(\vec{1}_{2 \times 3}) = \text{order}(\vec{2}_{2 \times 3}) = 7$. In general, we do not know which case will hold in part 3 of Proposition 5.1. \square

Table 1 records the order of $\vec{2}_{m \times n}$ for $m, n \in \{2, 3, \dots, 10\}$. Perhaps the most

$m \setminus n$	2	3	4	5	6	7	8	9	10
2	1	7	5	9	13	47	17	123	89
3	.	8	71	679	769	3713	8449	81767	93127
4	.	.	3	77	281	4271	2245	8569	18061
5	.	.	.	52	17753	726433	33507	24852386	20721019
6	29	434657	167089	265721	4213133
7	272	46069729	8118481057	4974089647
8	901	190818387	1031151241
9	73124	1234496016491
10	89893

TABLE 1. Order of the all-2s element on $\text{SF}_{m \times n}$ (symmetric in m and n).

striking feature of Table 1 is the relatively small size of the numbers along the diagonal ($m = n$). It seems natural to group these according to parity. The sequence $\{\vec{2}_{2n \times 2n}\}_{n \geq 1}$ starts 1, 3, 29, 901, 89893, \dots , which is the beginning of the famous sequence, $(a_n)_{n \geq 1}$, we now describe. The following was established independently by several people (cf. [17]):

Proposition 5.3. *The number of domino tilings of a $2n \times 2n$ checkerboard has the form*

$$2^n a_n^2$$

where a_n is an odd integer.

For each positive integer n , let P_n be the sandpile graph with vertices

$$V(P_n) = \{v_{i,j} : 1 \leq i \leq n \text{ and } 1 \leq j \leq i\} \cup \{s\}.$$

Each $v_{i,j}$ is connected to those vertices $v_{i',j'}$ such that $|i - i'| + |j - j'| = 1$. In addition, every vertex of the form $v_{i,n}$ is connected to the sink vertex, s . The

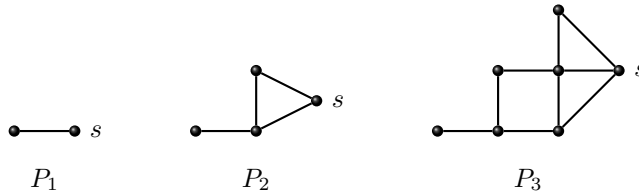


FIGURE 20.

first few cases are illustrated in Figure 20. Next define a family of triangular checkerboards, H_n , as in Figure 21. The checkerboard H_n for $n \geq 2$ is formed by adding a $2 \times (2n - 1)$ array (width-by-height) of squares to the right of H_{n-1} . These graphs were introduced by M. Ciucu [5] and later used by L. Pachter [6] to

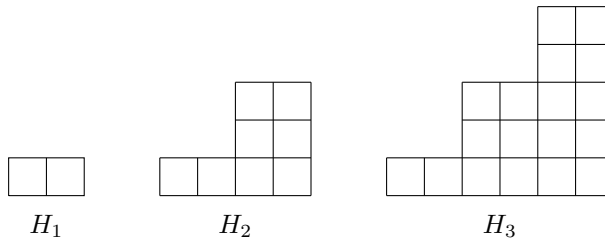


FIGURE 21.

give the first combinatorial proof of Proposition 5.3. As part of his proof, Pachter shows that a_n is the number of domino tilings of H_n .

As noted in [19], considering H_n as a planar graph and taking its dual (forgetting about the unbounded face of H_n) gives the graph $\mathcal{H}(P_n)$ corresponding to P_n under the generalized Temperley bijection of Section 3. See Figure 22.

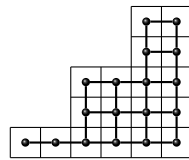


FIGURE 22. H_3 and $\mathcal{H}(P_3)$.

Proposition 5.4. *The number of elements in the sandpile group for P_n is*

$$\# \mathcal{S}(P_n) = a_n,$$

where a_n is as in Proposition 5.3.

Proof. The number of domino tilings of H_n equals the number of perfect matchings of $\mathcal{H}(P_n)$. By the generalized Temperley bijection, the latter is the number of spanning trees of P_n , and hence, the order of the sandpile group of P_n . As mentioned above, Pachter shows in [6] that a_n is the number of domino tilings of H_n . \square

The main result of this section is the following:

Theorem 5.5. *Let $\langle \vec{2}_{2n \times 2n} \rangle$ be the cyclic subgroup of $\mathcal{S}(\text{S}\Gamma_{2n \times 2n})$ generated by the all-2s element of $\Gamma_{2n \times 2n}$, and let $\vec{2}_n$ denote the all-2s element on P_n . Then the mapping*

$$\psi: \langle \vec{2}_{2n \times 2n} \rangle \rightarrow \mathcal{S}(P_n),$$

determined by $\psi(\vec{2}_{2n \times 2n}) = \vec{2}_n$, is a well-defined injection of groups.

Proof. Let \tilde{V}_n and $\tilde{V}_{2n \times 2n}$ denote the non-sink vertices of P_n and $\text{S}\Gamma_{2n \times 2n}$, respectively. We view configurations on P_n as triangular arrays of natural numbers and configurations on $\text{S}\Gamma_{2n \times 2n}$ as $2n \times 2n$ square arrays of natural numbers. Divide the $2n \times 2n$ grid by drawing bisecting horizontal, vertical, and diagonal lines, creating eight wedges. Define $\phi: \mathbb{Z}\tilde{V}_n \rightarrow \mathbb{Z}\tilde{V}_{2n \times 2n}$, by placing a triangular array in the position of one of these wedges, then flipping about lines, creating a configuration on $\text{S}\Gamma_{2n \times 2n}$ with dihedral symmetry. Figure 23 illustrates the case $n = 4$.

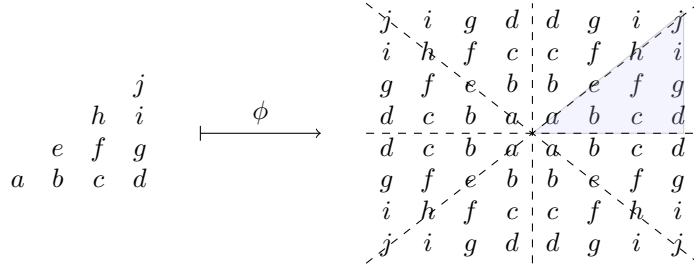


FIGURE 23. $\phi: \mathbb{Z}P_4 \rightarrow \mathbb{Z}\text{S}\Gamma_{8 \times 8}$.

We define special types of configurations on P_n . First, let s_n be the configuration in which the number of grains of sand on each vertex records that vertex's distance to the sink; then let t_n denote the sandpile with no sand except for one grain on each vertex along the boundary diagonal, i.e., those vertices with degree less than 3. Figure 24 illustrates the case $n = 4$.

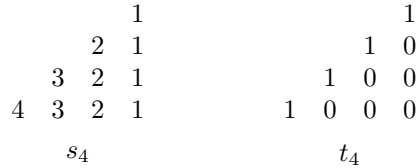


FIGURE 24. Special configurations on P_4 .

Let $\tilde{\Delta}_n$ and $\tilde{\Delta}_{2n \times 2n}$ be the reduced Laplacians for P_n and $\text{S}\Gamma_{2n \times 2n}$, respectively. The following are straightforward calculations:

- (1) $\tilde{\Delta}_n s_n = t_n$.
- (2) If $c \in \mathbb{Z}P_n$, then $\tilde{\Delta}_{2n \times 2n}(\phi(c))$ equals $\phi(\tilde{\Delta}_n(c))$ at all non-sink vertices of $\text{S}\Gamma_{2n \times 2n}$ except along the diagonal and anti-diagonal, where they differ by a factor of 2:

$$\tilde{\Delta}_{2n \times 2n}(\phi(c))_{ij} = \begin{cases} 2\phi(\tilde{\Delta}_n(c))_{ij} & \text{for } i = j \text{ or } i + j = 2n + 1, \\ \phi(\tilde{\Delta}_n(c))_{ij} & \text{otherwise.} \end{cases}$$

Let $\tilde{\mathcal{L}}_n \subset \mathbb{Z}V_n$ and $\tilde{\mathcal{L}}_{2n \times 2n} \subset \mathbb{Z}V_{2n \times 2n}$ denote the images of $\tilde{\Delta}_n$ and $\tilde{\Delta}_{2n \times 2n}$, respectively. Identify the sandpile groups of P_n and $\text{ST}_{2n \times 2n}$ with $\mathbb{Z}V_n/\tilde{\mathcal{L}}_n$ and $\mathbb{Z}V_{2n \times 2n}/\tilde{\mathcal{L}}_{2n \times 2n}$, respectively. To show that ψ is well-defined and injective, we need to show that $k\vec{2}_n \in \tilde{\mathcal{L}}_n$ for some integer k if and only if $k\vec{2}_{2n \times 2n} \in \tilde{\mathcal{L}}_{2n \times 2n}$. Since the reduced Laplacians are invertible over \mathbb{Q} , there exist unique vectors x and y defined over the rationals such that

$$\tilde{\Delta}_n x = \vec{2}_n \quad \text{and} \quad \tilde{\Delta}_{2n \times 2n} y = \vec{2}_{2n \times 2n}.$$

Using the special configurations s_n and t_n and the two calculations noted above,

$$\tilde{\Delta}_n x = \vec{2}_n \implies \tilde{\Delta}_n(x - s_n) = \vec{2}_n - t_n \implies \tilde{\Delta}_{2n \times 2n} \phi(x - s_n) = \vec{2}_{2n \times 2n}.$$

In other words,

$$(5.2) \quad y = \phi(x - s_n).$$

Using the fact that $\tilde{\Delta}_n$ is invertible over \mathbb{Q} , we see that $k\vec{2}_n \in \tilde{\mathcal{L}}_n$ if and only if kx has integer coordinates. By (5.2), this is the same as saying ky has integer components, which in turn is equivalent to $k\vec{2}_{2n \times 2n} \in \tilde{\mathcal{L}}_{2n \times 2n}$, as required. \square

Combining this result with Proposition 5.4 gives

Corollary 5.6. *The order of $\vec{2}_{2n \times 2n}$ divides a_n .*

6. CONCLUSION

We conclude with a list of suggestions for further work.

1. Theorem 4.5 states that the number of domino tilings of a Möbius checkerboard equals the number of domino tilings of an associated ordinary checkerboard after assigning weights to certain domino positions. We would like to see a direct bijective proof—one that does not rely on the Lu-Wu formula (and thus giving a new proof of that formula). For instance, consider the tiling of the 4×4 checkerboard that appears second in the top row of Figure 8. It has one domino of weight 2. So this weighted tiling should correspond to two tilings of the 4×4 Möbius checkerboard. Presumably, one of these two tilings is just the unweighted version of the given tiling. One might imagine that the other tiling would result from pushing the single blue domino to the right one square so that it now wraps around on the Möbius checkerboard, and then making room for this displacement by systematically shifting the other dominos.
2. Section 5 is motivated by Irena Swanson's question: what is the order of the all-1s configuration, $\vec{1}_{m \times n}$, on the $m \times n$ sandpile grid graph? Proposition 5.1 (3) shows this order is either the same as or twice the order of the all-2s configuration, $\vec{2}_{m \times n}$. It would be nice to know when each case holds. Corollary 5.6 says the order of $\vec{2}_{2n \times 2n}$ divides the integer a_n of Proposition 5.3, connected with domino tilings. When is this order equal to a_n ? Ultimately, of course, we would like to know the answer to Swanson's original question.
3. Example 4.3 introduces an action of the sandpile group of the $2m \times 2n$ sandpile grid graph on the domino tilings of the $2m \times 2n$ checkerboard. Perhaps this group action deserves further study.
4. To summarize some of the main ideas of this paper, suppose a group acts on an arbitrary sandpile graph Γ . If the corresponding symmetrized reduced Laplacian or its transpose is the (ordinary) reduced Laplacian of a sandpile graph Γ' , then

Proposition 2.10 yields a group isomorphism between the symmetric configurations on Γ and the sandpile group $\mathcal{S}(\Gamma')$ of Γ' . By the matrix-tree theorem, the size of the latter group is the number of spanning trees of Γ' (and, in fact, as mentioned earlier, $\mathcal{S}\Gamma'$ is well-known to act freely and transitively on the set of spanning trees of Γ'). The generalized Temperley bijection then gives a correspondence between the spanning trees of Γ' and perfect matchings of a corresponding graph, $\mathcal{H}(\Gamma')$. Thus, the number of symmetric recurrents on Γ equals the number of perfect matchings of $\mathcal{H}(\Gamma')$. We have applied this idea to the case of a particular group acting on sandpile grid graphs. Does it lead to anything interesting when applied to other classes of graphs with group action? The Bachelor's thesis of the first author [13] includes a discussion of the case of a dihedral action on sandpile grid graphs.

REFERENCES

- [1] Per Bak, Chao Tang, and Kurt Wiesenfeld, *Self-Organized Criticality: An Explanation of $1/f$ Noise*, Phys. Rev. Lett. **59** (1987), no. 4, 381–384.
- [2] Matthew Baker and Serguei Norine, *Riemann-Roch and Abel-Jacobi theory on a finite graph*, Adv. Math. **215** (2007), no. 2, 766–788.
- [3] Matthew Baker and Farbod Shokrieh, *Chip-firing games, potential theory on graphs, and spanning trees*, J. Combin. Theory Ser. A **120** (2013), no. 1, 164–182.
- [4] Norman Biggs, *Algebraic potential theory on graphs*, Bull. London Math. Soc. **29** (1997), no. 6, 641–682.
- [5] Mihai Ciucu, Weigen Yan, and Fuji Zhang, *The number of spanning trees of plane graphs with reflective symmetry*, J. Combin. Theory Ser. A **112** (2005), no. 1, 105–116.
- [6] ———, *The number of spanning trees of plane graphs with reflective symmetry*, J. Combin. Theory Ser. A **112** (2005), no. 1, 105–116.
- [7] F. Cools, J. Draisma, S. Payne, and E. Robeva, *A tropical proof of the Brill-Noether Theorem*, Adv. Math. **230** (2012), 759–776.
- [8] Deepak Dhar, *Self-organized critical state of sandpile automaton models*, Phys. Rev. Lett. **64** (1990), no. 14, 1613–1616.
- [9] ———, *Theoretical studies of self-organized criticality*, Phys. A **369** (2006), no. 1, 29–70.
- [10] Anton Dochtermann and Raman Sanyal, *Laplacian ideals, arrangements, and resolutions*, eprint, [arXiv:1212.6244](https://arxiv.org/abs/1212.6244), to appear in J. Algebraic Combin.
- [11] Natalie J. Durgin, *Abelian Sandpile Model on Symmetric Graphs*, Bachelor's thesis, Harvey Mudd College, 2009.
- [12] Anne Fey, Lionel Levine, and David B. Wilson, *Approach to criticality in sandpiles*, Phys. Rev. E (3) **82** (2010), no. 3, 031121, 14.
- [13] Laura Florescu, *New connections between the Abelian Sandpile Model and domino tilings*, Bachelor's thesis, Reed College, 2011.
- [14] Alexander E. Holroyd, Lionel Levine, Karola Mészáros, Yuval Peres, James Propp, and David B. Wilson, *Chip-firing and rotor-routing on directed graphs*, In and out of equilibrium. 2, Progr. Probab., vol. 60, Birkhäuser, Basel, 2008, pp. 331–364.
- [15] Sam Hopkins and David Perkinson, *Biographical Arrangements*, eprint, [arXiv:1212.4398](https://arxiv.org/abs/1212.4398), to appear in Trans. Amer. Math. Soc.
- [16] ———, *Orientations, semiorders, arrangements, and parking functions*, Elec. J. of Combin. **19** (2012), no. 4.
- [17] P. John, H. Sachs, and H. Zernitz, *Problem 5. Domino Covers in Square Chessboards*, Zastosowania Matematyki (Applicationes Mathematicae) **XIX** (1987), no. 3–4, 635–641.
- [18] P. W. Kasteleyn, *The statistics of dimers on a lattice, I. the number of dimer arrangements on a quadratic lattice*, Physica **27** (1961), 1209–1225.
- [19] Richard W. Kenyon, James G. Propp, and David B. Wilson, *Trees and matchings*, Electron. J. Combin. **7** (2000), Research Paper 25, 34 pp. (electronic).
- [20] Lionel Levine and Yuval Peres, *Strong spherical asymptotics for rotor-router aggregation and the divisible sandpile*, Potential Anal. **30** (2009), no. 1, 1–27.
- [21] Wentao T. Lu and F. Y. Wu, *Close-packed dimers on nonorientable surfaces*, Phys. Lett. A **293** (2002), no. 5-6, 235–246.

- [22] Madhusudan Manjunath, Frakn-Olaf Schreyer, and John Wilmes, *Minimal Free Resolutions of the g -Parking Function Ideal and the Toppling Ideal*, eprint, [arXiv:1210.7569](https://arxiv.org/abs/1210.7569), to appear in Trans. Amer. Math. Soc.
- [23] Madhusudan Manjunath and Bernd Sturmfels, *Monomials, binomials and Riemann-Roch*, J. Algebraic Combin. **37** (2013), no. 4, 737–756.
- [24] Sergei Maslov, *Sandpile applet*, <http://www.cmth.bnl.gov/~maslov/Sandpile.htm>, Online: accessed 22-May-2014.
- [25] J. C. Mason and D. C. Handscomb, *Chebyshev polynomials*, Chapman & Hall/CRC, Boca Raton, FL, 2003.
- [26] Criel Merino López, *Chip firing and the Tutte polynomial*, Ann. Comb. **1** (1997), no. 3, 253–259.
- [27] Luca Guido Molinari, *Determinants of block tridiagonal matrices*, Linear Algebra and its Applications **429** (2008), 22212226.
- [28] Gregg Musiker, *The critical groups of a family of graphs and elliptic curves over finite fields*, J. Algebraic Combin. **30** (2009), no. 2, 255–276.
- [29] *The On-Line Encyclopedia of Integer Sequences*, A067502, oeis.org/A081567.
- [30] S. Ostojic, *Patterns formed by addition of grains to only one site of an abelian sandpile.*, Phys. A **318** (2003), 187–199.
- [31] Guglielmo Paoletti, *Deterministic Abelian Sandpile Models and Patterns*, Ph.D. thesis, Università di Pisa, 2012.
- [32] Wesley Pegden and Charles K Smart, *Apollonian structure in the Abelian Sandpile*, eprint, [arXiv:1208.4839](https://arxiv.org/abs/1208.4839), 2012.
- [33] Wesley Pegden and Charles K. Smart, *Convergence of the Abelian sandpile*, Duke Math. J. **162** (2013), no. 4, 627–642.
- [34] David Perkinson, Jacob Perlman, and John Wilmes, *Primer for the algebraic geometry of sandpiles*, Tropical and Non-Archimedean Geometry, Contemp. Math., vol. 605, Amer. Math. Soc., Providence, RI, 2013, pp. 211–256.
- [35] Alexander Postnikov and Boris Shapiro, *Trees, parking functions, syzygies, and deformations of monomial ideals*, Trans. Amer. Math. Soc. **356** (2004), no. 8, 3109–3142 (electronic).
- [36] Tridib Sadhu and Deepak Dhar, *Pattern formation in growing sandpiles with multiple sources or sinks*, J. Stat. Phys. **138** (2010), no. 4-5, 815–837.
- [37] Eugene Speer, *Asymmetric abelian sandpile models*, J. Stat. Phys. (1993), 61–74.
- [38] W. A. Stein et al., *Sage Mathematics Software (Version 5.1)*, The Sage Development Team, 2012, <http://www.sagemath.org>.
- [39] H. N. V. Temperley and Michael E. Fisher, *Dimer problem in statistical mechanics—an exact result*, Philos. Mag. (8) **6** (1961), 1061–1063.
- [40] Wikipedia, *Chebyshev polynomials* — *Wikipedia, the free encyclopedia*, 2012, [Online; accessed 22-May-2014].

COURANT INSTITUTE, NYU, NEW YORK
E-mail address: florescu@cims.nyu.edu

DEPARTMENT OF ECONOMICS, UNIVERSITY OF MICHIGAN, ANN ARBOR
E-mail address: morard@umich.edu

DEPARTMENT OF MATHEMATICS, REED COLLEGE
E-mail address: davidp@reed.edu

DEPARTMENT OF MATHEMATICS, UNIVERSITY OF CHICAGO
E-mail address: nks@math.uchicago.edu

DEPARTMENT OF MATHEMATICS, UNIVERSITY OF OREGON
E-mail address: tianyuan@uoregon.edu